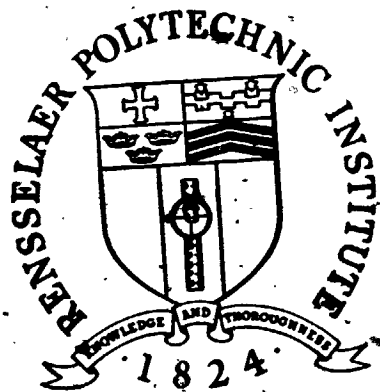


(NASA-19-104202) DESIGN AND EVALUATION OF A
TORSIONAL WHEEL FOR PLANETARY PROBES
(Rensselaer Polytechnic Inst., Troy, N. Y.)
97 p HC A05/MF A01 CSCL 131

N78-10471

Unclass
50758

33/37



Rensselaer Polytechnic Institute

Troy, New York 12181

RPI TECHNICAL REPORT MP-53

DESIGN AND EVALUATION OF A
TOROIDAL WHEEL FOR PLANETARY ROVERS

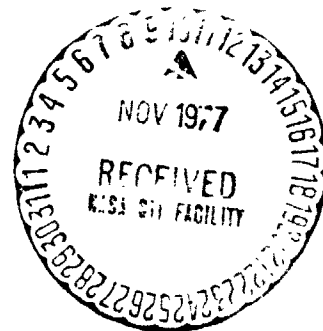
A STUDY SUPPORTED BY THE
NATIONAL AERONAUTICS AND SPACE
ADMINISTRATION

GRANT NGL 33-018-081

Joseph Koskol
Stephen Yerazunis

School of Engineering
Rensselaer Polytechnic Institute

October 1977



LIST OF FIGURES

		Page
FIGURE 1	LOCKHEED ELASTIC MOBILITY SYSTEM	2
FIGURE 2	ORIGINAL TOROIDAL WHEEL	5
FIGURE 3	STANDARD TOROIDAL WHEEL	6
FIGURE 4	STATIC HOOP TESTER	8
FIGURE 5	STANDARD HOOP - UNLOADED	13
FIGURE 6	STANDARD HOOP - COMPRESSED	14
FIGURE 7	STANDARD HOOP - DEFLECTED	15
FIGURE 8	STANDARD HOOP - TYPICAL FAILURE	17
FIGURE 9	OFFSET STANDARD HOOP	18
FIGURE 10	INVERTED HOOP - UNLOADED	20
FIGURE 11	INVERTED HOOP - COMPRESSED	21
FIGURE 12	INVERTED HOOP - DEFLECTED	22
FIGURE 13	LOADING CHARACTERISTICS OF THE STANDARD AND INVERTED WHEELS	24
FIGURE 14	TRACTION TESTER	25
FIGURE 15	STANDARD WHEEL - DEFLECTION CALIBRATION . . .	27
FIGURE 16	INVERTED WHEEL - DEFLECTION CALIBRATION . . .	28
FIGURE 17	DEFLECTION AS A FUNCTION OF LOAD	29
FIGURE 18	NET GROUND THRUST AS A FUNCTION OF LOAD . . .	30
FIGURE 19	STANDARD WHEEL - ENDURANCE TESTING	31
FIGURE 20	INVERTED WHEEL - ENDURANCE TESTING	32
FIGURE 21	VIBRATION TESTER	33
FIGURE 22	HOOP - SPOKE STRESS CONCENTRATION	35
FIGURE 23	INVERTED HOOP EMPLOYING THE STRESS DISTRIBUTION PLATE	36

FIGURE 24	GROUSER ATTACHMENT	37
FIGURE 25	STATIC CONDITION	39
FIGURE 26	A,B INVERTED HOOP - FREE BODY DIAGRAMS	41
FIGURE 27	INVERTED HOOP - FREE BODY DIAGRAM	43
FIGURE 28	INVERTED WHEEL UNDER COMPRESSION	45
FIGURE 29	MULTIPLE BAND INVERTED HOOP	48
FIGURE 30	S - N DIAGRAM FOR STEEL	58
FIGURE 31	GOODMAN DIAGRAM	59
FIGURE 32	R.P.I. MARS ROVING VEHICLE	62

LIST OF TABLES

		Page
TABLE 1	INVERTED TOROIDAL WHEEL PROGRAM - SAMPLE OUTPUT	49
TABLE 2	BANDS PROGRAM - SAMPLE OUTPUT	52
TABLE 3	THEORETICAL vs. EXPERIMENTAL HOOPS . .	53
TABLE 4	THEORETICAL vs. EXPERIMENTAL WHEEL . .	54
TABLE 5	WHEELS FOR THE RPI ROVER - STEEL . . .	63
TABLE 6	WHEELS FOR THE RPI ROVER - TITANIUM . .	65
TABLE 7	WHEELS FOR THE RPI ROVER - S-GLASS . .	67
TABLE 8	WHEELS FOR THE PROPOSED ROVER - TITANIUM	71
TABLE 9	WHEELS FOR THE PROPOSED ROVER - S-GLASS	75

SYMBOLIC NOTATION

A_F	FOOTPRINT AREA
B	SPOKE BASE LENGTH
B_N	NUMBER OF BANDS PER HOOP
c	COEFFICIENT OF SOIL COHESION
C	STATIC HOOP CLEARANCE
C_0	NO-LOAD CLEARANCE
F	WHEEL THRUST
H	HOOP HEIGHT
I	AREA MOMENT OF INERTIA
K	HOOP SPRING CONSTANT
L	HOOP BAND LENGTH
L_A	AXLE LOAD
L_F	FOOTPRINT LENGTH
L_H	STATIC HOOP LOAD
L_W	STATIC WHEEL LOAD
M	BENDING MOMENT
N	NORMAL LOAD
N_1, N_c	SOIL COEFFICIENTS
P	HOOP LOAD
P_A	AVERAGE FOOTPRINT PRESSURE
R_H	AVERAGE HOOP RADIUS
R_W	WHEEL RADIUS
$R_{1,2,3}$	MOTION RESISTANCES
S	SPOKE FLANGE LENGTH
t	HOOP BAND THICKNESS
T	STATIC HOOP TENSION
w	HOOP BAND WIDTH
w_F	FOOTPRINT WIDTH
w_H	HOOP WIDTH
w_W	WHEEL WEIGHT
γ	SOIL DENSITY

δ_n
 r
 θ
 ρ
 ϕ

DEFLECTION OF HOOP N
SAFETY FACTOR
SPOKE FLANGE ANGLE
MATERIAL DENSITY
ANGLE OF SOIL FRICTION

ABSTRACT

A new mobility concept, called the "Inverted Toroidal Wheel", has been perceived, mathematically quantified, and experimentally verified. This wheel design has a number of important characteristics, namely; the low footprint pressures required for Mars exploration (0.5 to 1.0 p.s.i.), high vehicle weight to wheel weight ratios capable of exceeding 10:1, extremely long cyclic durances tending towards infinite life, and simplicity of design. This concept, in combination with appropriate materials such as Titanium or composites, can provide a planetary roving vehicle with a very high degree of exploratory mobility, a substantial savings in weight and a high assurity of mission success. The design equations and computation procedures necessary to formulate an inverted wheel are described in detail.

PRECEDING PAGE BLANK NOT FILMED

PART 1

INTRODUCTION AND HISTORICAL REVIEW

One of man's first and most important inventions was the wheel. Yet, even though this device has been with us through the ages, little has been done to improve its basic concept. Barring pneumatic tires and various track devices one could say that there has not been any changes since the wooden wheel.

The cause of this seems to lie in the fact that it is easier to build a road than to modify a wheel. This is evidenced in the millions of miles of rail and pavement worldwide. The first departure from this trend was precipitated by experiences during World War II when ordinary wheels were found to be ineffective in harsh terrains. A look at wheel shape and size resulted in much modification and various hybrid vehicles such as the half-track.

At this point in time, the inspiration for superior wheel and track designs comes from the Mars mission which is proposed for the 1980's. The stationary landers associated with the Viking program were only the first step. A more thorough investigation of Mars will require autonomous rovers of exceptional mobility for a broad range of terrains. A propulsive device capable of developing an average footprint pressure in the 0.5 to 1.0 p.s.i. range, which is much too low for a conventional wheel, is essential.

One device which might meet these special needs is the Lockheed Elastic Mobility System (LEMS), shown in Figure 1. This device has a very large footprint area which makes low footprint pressures possible. Two drawbacks exist with this system. Being a track device, it is much more complex than any wheel. Because of their low profile the risk of

ORIGINAL PAGE IS
OF POOR QUALITY

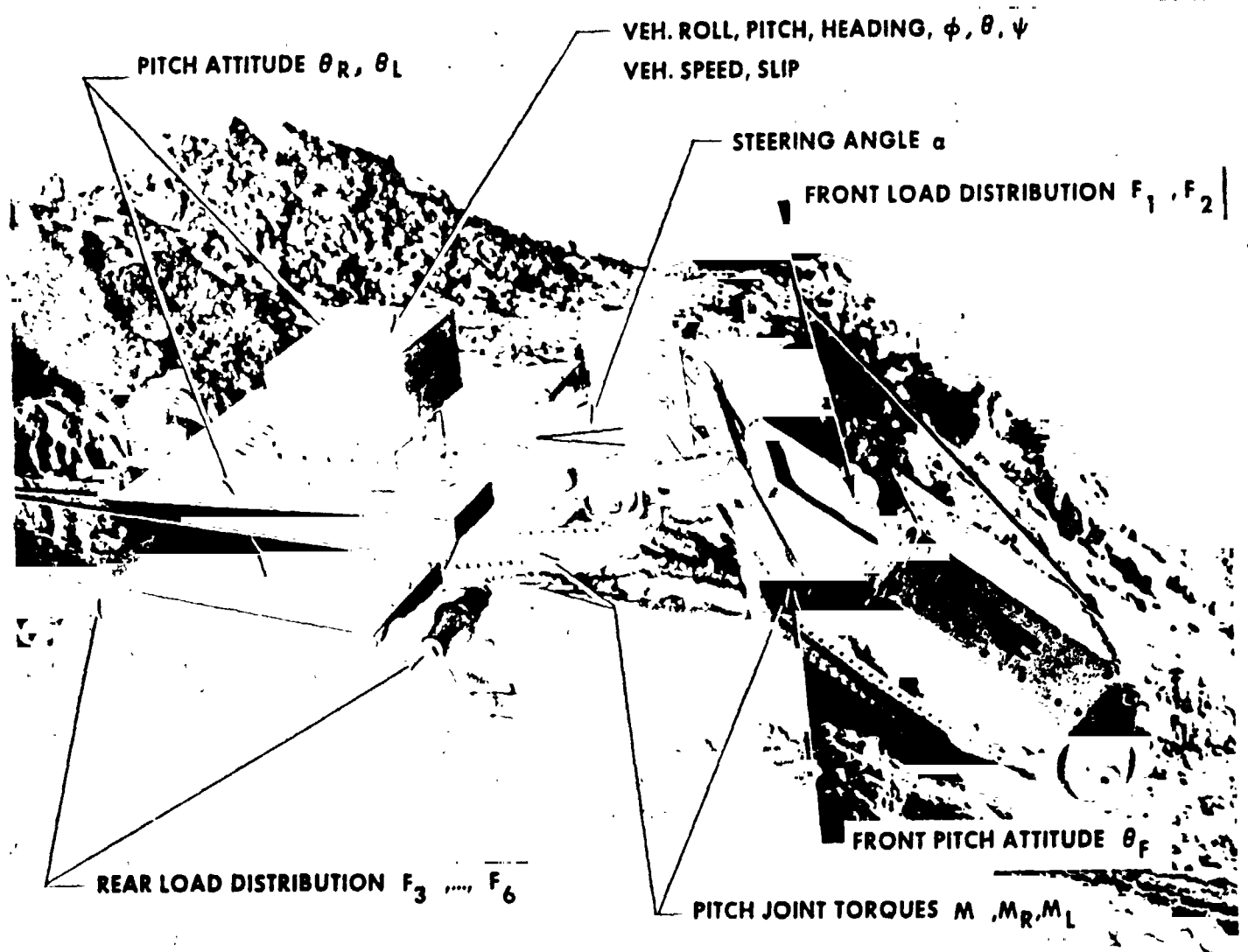


FIGURE 1

LOCKHEED ELASTIC MOBILITY SYSTEM

entrapment; i.e. the lodging of a track in a crevice or between small boulders; runs high. Under these circumstances, due to the manner of scuff steering required, breakaway would be difficult whereas a wheel might envelope the obstacle and free the vehicle.

A new wheel concept has been developed at Rensselaer and is described herein. The wheel is not only characterized by low footprint pressures but also by a high payload to wheel weight ration, exceptional traction and extreme simplicity.

PART 2

PRIOR INVESTIGATIONS

2.1 Mechanical Design Aspects

The original concept for a planetary wheel design was due to the work of R. Simon, reference 1. This concept employs elastic steel hoops fixed to an inner hub with an outer circumferential band attached through polymeric hinges. Figure 2 depicts what has come to be known as the toroidal wheel. Using various mathematical techniques, Simon attempted to quantify this concept. Subsequent years were spent reshaping the mathematical model in an attempt to obtain an exact solution which could then serve as a basis for the rational design and optimization of the wheel. Unfortunately, the several resulting mathematical models which were studied were found to possess serious limitations because of the assumptions required to permit analytical solutions. While the models were helpful in suggesting general design parameters, they did not reveal shortcomings which were perceived later in actual testing.

Turning to experimentation it was discovered that the circumferential band was the cause of poor footprint pressure. Upon its removal a much more promising wheel results. The addition of a spoke further increases the footprint area upon compression. Shown in Figure 3, is what is now referred to as the standard toroidal wheel. Studies were continued along the experimental viewpoint by R. Lipowicz, reference 2. The major thrust was aimed at correlating numerous curves of deflection as a function of load. The curves were generated via the static hoop



FIGURE 2

ORIGINAL TOROIDAL WHEEL

ORIGINAL PAGE IS
OF POOR QUALITY

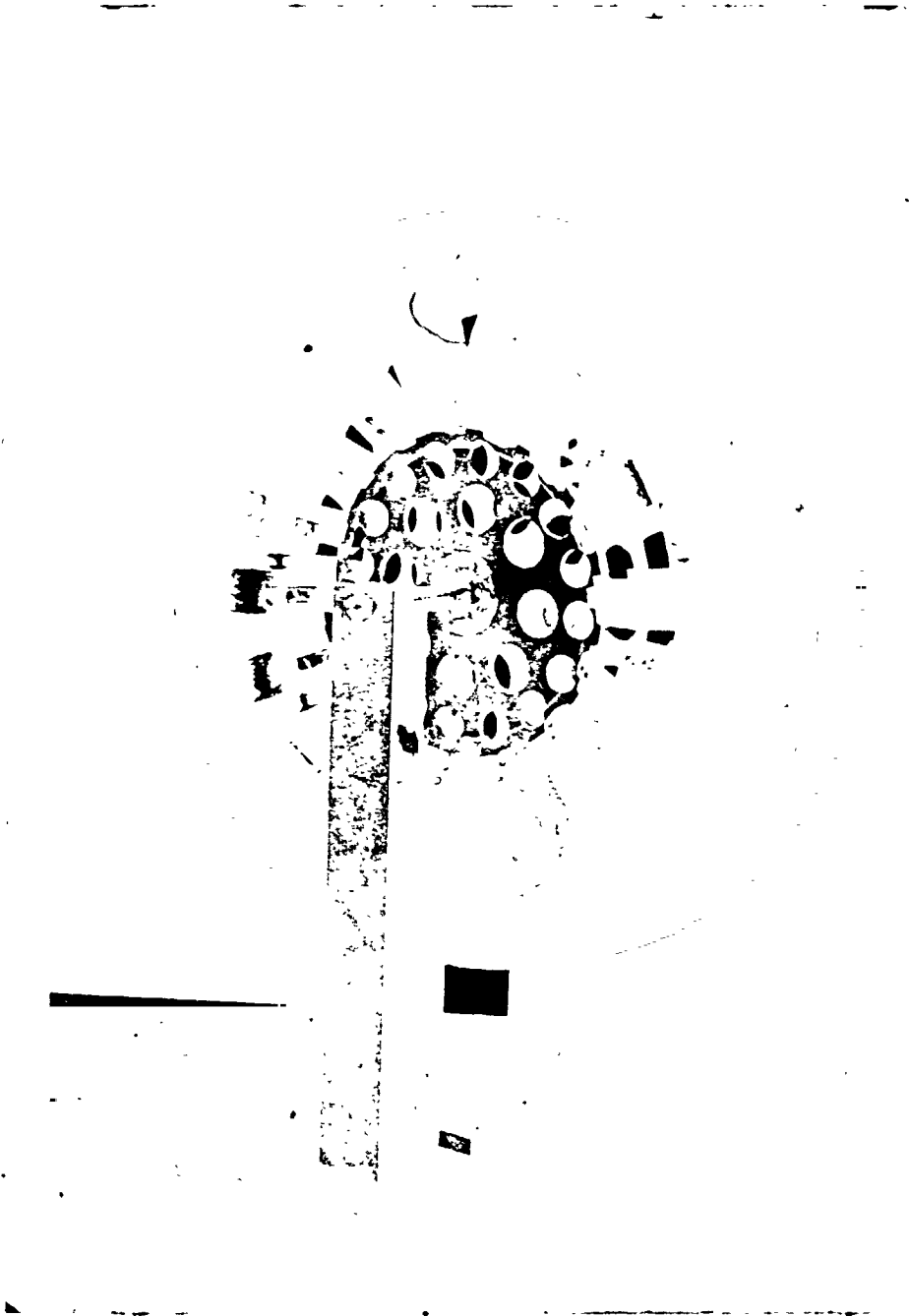


FIGURE 3

STANDARD TOROIDAL WHEEL

tester shown in Figure 4. Although much data was tabulated, no general design technique was procured.

2.2 Soil Interfacing Aspects

Lipowicz also recognized the importance of wheel/soil relationships. What he realized was that in order to design a wheel, one must understand the character of the soil in which the wheel is expected to function. Knowing the soil parameters one may thereby find the dimensions defining the optimum wheel for that soil. For planetary exploration this would be a fruitless effort, for as a vehicle attempts to traverse 100 or more kilometers of terrain, the wheel will encounter many varied soil characteristics. However one should not go so far as to neglect the soil equations altogether since they guide a design along the proper path. The following arguments are therefore meant to provide a qualitative guideline.

A wheel is expected to perform two tasks. It is to provide thrust to the vehicle by shearing the soil and it must provide floatation which is the ability of a vehicle to remain on the ground surface. To understand these phenomenon, the two soil extremes, frictional and cohesive soils, must be considered.

A frictional soil is one such as dry sand. Thrust is developed by packing the grains together and, according to Coulombs' law of friction, is expressed by,

$$F = W \tan \phi$$
 2.2.1

One can therefore see that for purely frictional soils the thrust, F,

ORIGINAL PAGE IS
OF POOR QUALITY

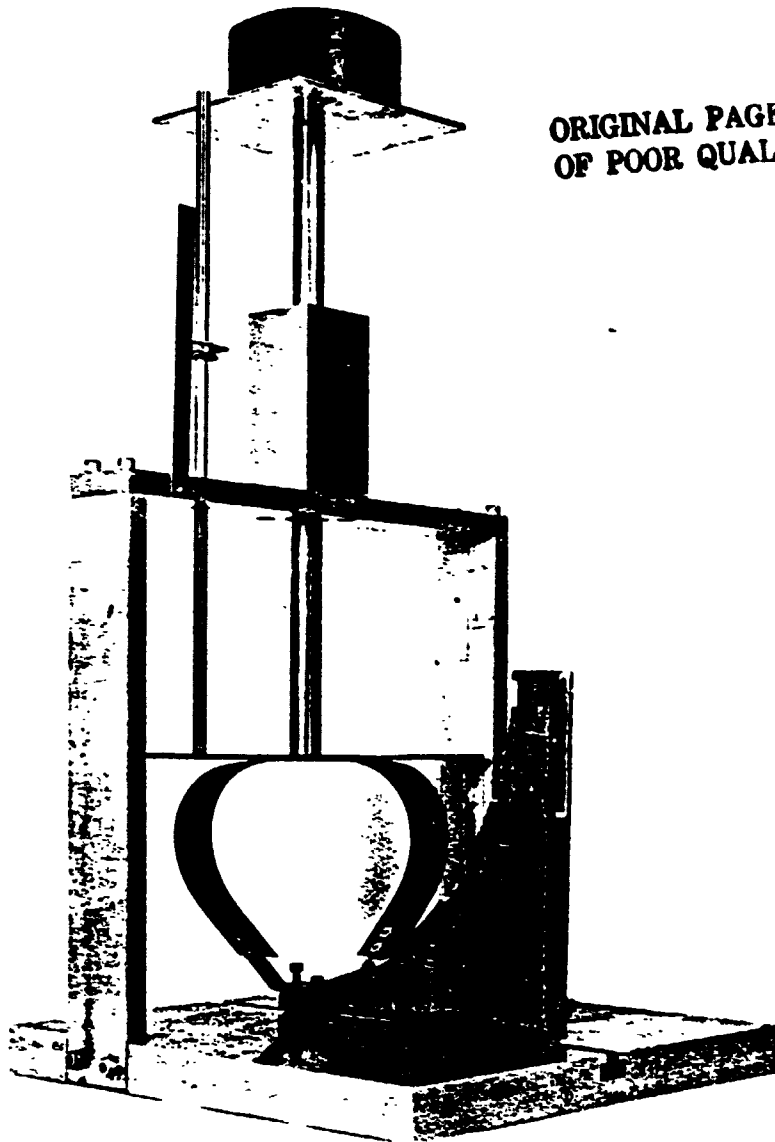


FIGURE 1

STATIC HOOP TESTER

is a function of the load applied to the wheel and the soil angle of friction, ϕ , which depends upon the soil itself. The ability of a wheel to float in frictional soils is expressed by,

$$W_s = 1/2 W_f^2 L_f \gamma N_\gamma \quad 2.2.2$$

This equation suggests that the safe load can be increased most effectively by increasing the width of the footprint and to a lesser extent by increasing the length of the footprint, where N_γ and γ are soil functions.

A cohesive soil is one such as wet clay. Thrust is developed by the adhesive action of the soil on the wheel. This thrust can be calculated from the equation,

$$F = A_f c \quad 2.2.3$$

which shows that the thrust is proportional to the footprint area and to the coefficient of soil cohesion. The ability of the wheel to float in cohesive soils is given as,

$$W_s = A_f c N_c \quad 2.2.4$$

Therefore, floatation is increased by a larger footprint area only, since c and N_c are soil parameters.

Combining these sets of equations one obtains the following equations which apply to any soil as,

$$F = W \tan \phi + W_f L_f c \quad 2.2.5$$

and,

$$W_s = 1/2 W_f L_f (W_f \gamma N_\gamma + 2 c N_c) \quad 2.2.6$$

where ϕ , c , γ , N_γ , and N_c must be determined experimentally for each soil considered.

From this set of equations it would appear that increasing the footprint width to the maximum would yield the best wheel. This would be true except for the fact that soil resistance has not yet been considered.

For any wheel there are three types of resistance to motion: bulldozing (R_1), compaction (R_2) and adhesion (R_3). Bulldozing resistance originates with the pushing by the wheel of soil in its path. Compaction resistance is caused by the packing of the soil under the wheel in front of the axle, while behind the axle adhesive resistance "glues" the wheel to the ground through the capillary action produced by cohesive soils. All of these resistances are a function of wheel width and increase with it. The total governing equations for wheel-soil interfacing are then,

$$F = W \tan \phi + W_f L_f c - (R_1 + R_2 + R_3) \quad 2.2.7$$

and,

$$W_s = 1/2 W_f L_f (W_f \gamma N_\gamma + 2cN_c) \quad 2.2.8$$

One is therefore faced with a trade-off. Again it must be stated that if a wheel were being designed for constant soil parameters then the optimum wheel dimensions could be found. Since an array of soil parameters will be met, one is forced to adopt a probabilistic standpoint.

Data of this sort was compiled by Martin-Marietta, Inc. with the resulting conclusion that for optimum overall exploratory mobility, with

due consideration for variations which range from a loess material to rocky terrains, one should design for an average footprint pressure between 0.5 to 1.0 p.s.i.

PART 3

DEFICIENCIES OF THE STANDARD TOROIDAL WHEEL LEAD TO NEW CONCEPTS

3.1 Shortcomings of the Standard Toroidal Wheel

Even though the standard toroidal wheel is far superior to its precursor they both possess the same three intrinsic faults, namely; high footprint pressure, lateral instability, and stress reversal.

The removal of the circumferential band was a correct step in reducing the footprint pressure of the toroidal wheel. Another measure might be to increase the overall wheel dimensions. But, with experimental wheels yielding footprint pressures of 1.75 p.s.i. when subjected to loads of only 40 lbs., a satisfactory wheel design begins to seem unlikely.

Due to the geometry of the standard hoop (Figure 5) when it is compressed (Figure 6) it is subjected to internal body forces which drive it away from its center (Figure 7). This is explained by the fact that the average radius of curvature in the on-center condition is less than in the off-center condition. Thus the energy level of the system which is expressed by:

$$U = \frac{1}{2EI} \int_S M^2 ds \quad 3.1.1$$

where,

$$M = \frac{EI}{R_H} \quad 3.1.2$$

is lower when the hoop is in the off-center position, and the hoop will therefore seek this configuration. This phenomenon leads to poor lateral stability and lower vehicle mobility on pitching and rolling terrains.

ORIGINAL PAGE IS
OF POOR QUALITY



FIGURE 5

STANDARD HOOP - UNLOADED

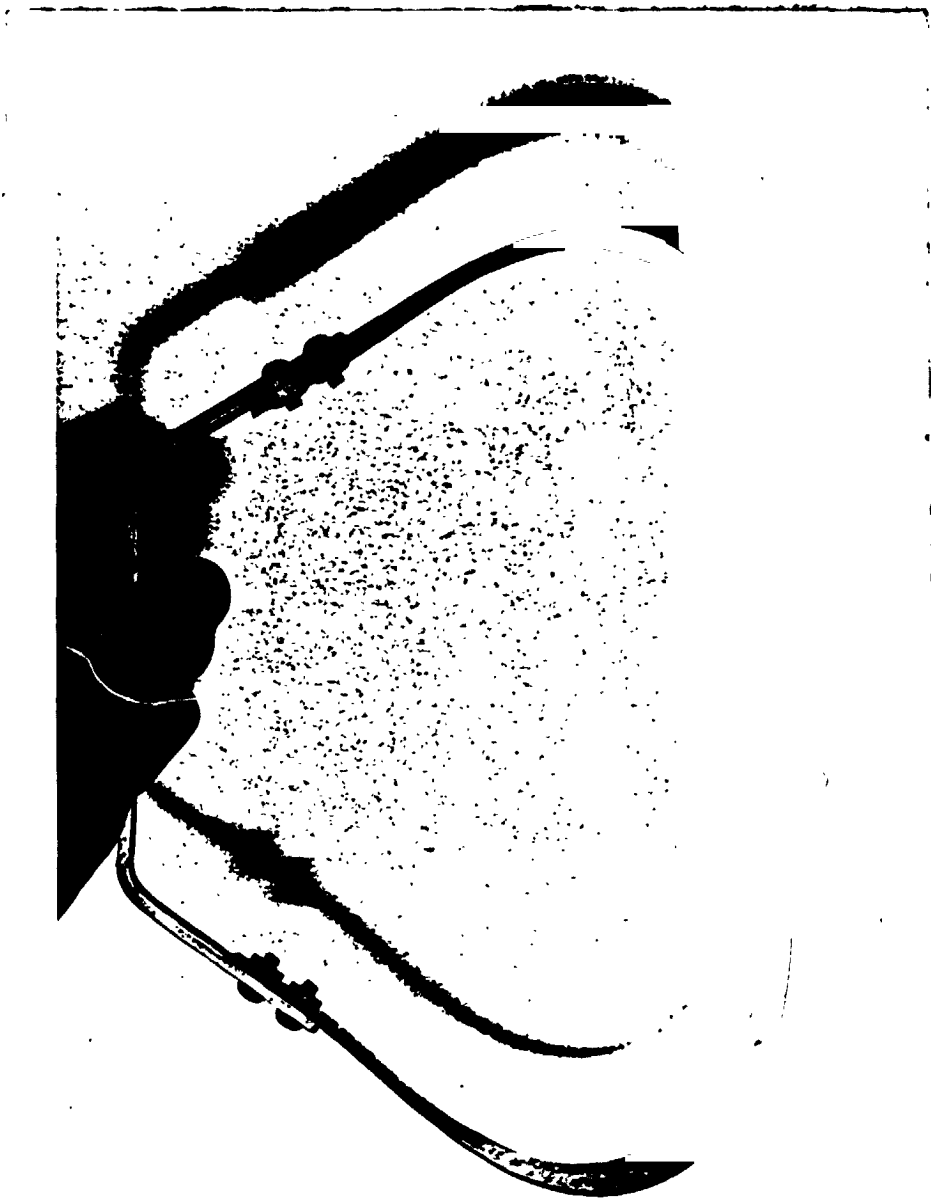


FIGURE 6

STANDARD HOOP - COMPRESSED



FIGURE 7

STANDARD HOOP - DEFLECTED

Examination of the geometry of the standard hoop in compression (Figure 6) reveals major changes in curvature. A radius of curvature equal to negative infinity exists at the spoke flange. This radius decreases in magnitude to some finite negative value and then returns to negative infinity as the inflection point is approached. Immediately beyond the inflection point the radius of curvature jumps to positive infinity. The radius then decreases to some finite positive radius of curvature and then returns to positive infinity as the hoop axis of symmetry is approached. The upper portion of the hoop; i.e. that portion existing between the flange and the inflection point, is subjected to reversals in bending moment upon compression and relaxation. This is therefore the expected area of failure. Experiment has shown this conclusion to be entirely correct. A typical failure is shown in Figure 8.

3.2 A New Outlook

Investigators in past years have tended to accept what existed previously and apply modifications which resulted in only minor improvements. As one would surmise from Section 3.1, the problem lies within the hoop itself. Once these deficiencies were isolated, the conclusion was drawn that a new outlook must be taken with respect to the hoop-spoke geometry. Several alternative concepts were perceived and explored as described below.

The instability of the standard hoop is somewhat lessened by the offsetting of the center lines of the spoke flanges with respect to one another. An offset standard hoop is shown in Figure 9. The effect that this has is to introduce a twisting energy, which increases as the hoop

ORIGINAL PAGE IS
OF POOR QUALITY

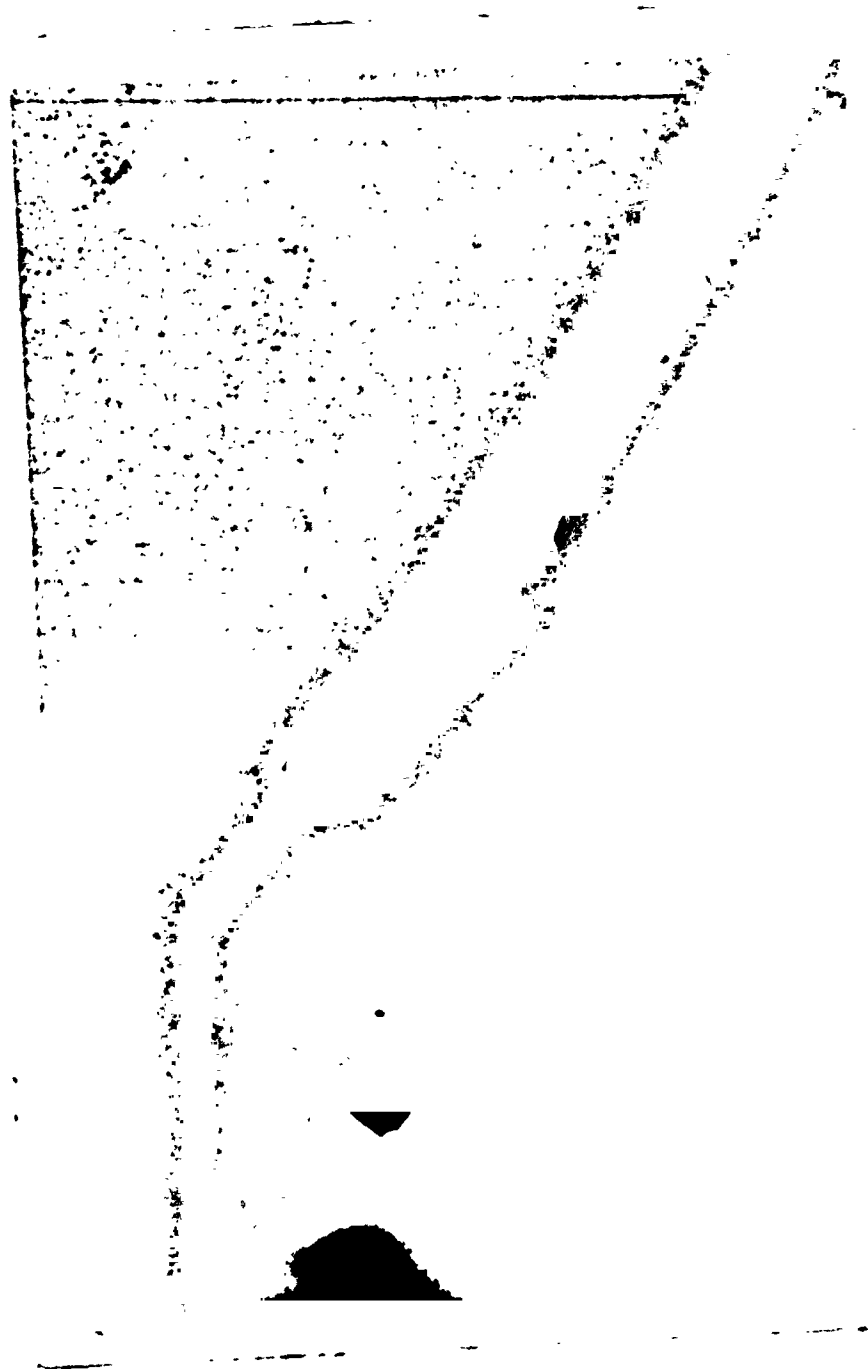


FIGURE 8

STANDARD HOOP - TYPICAL FAILURE

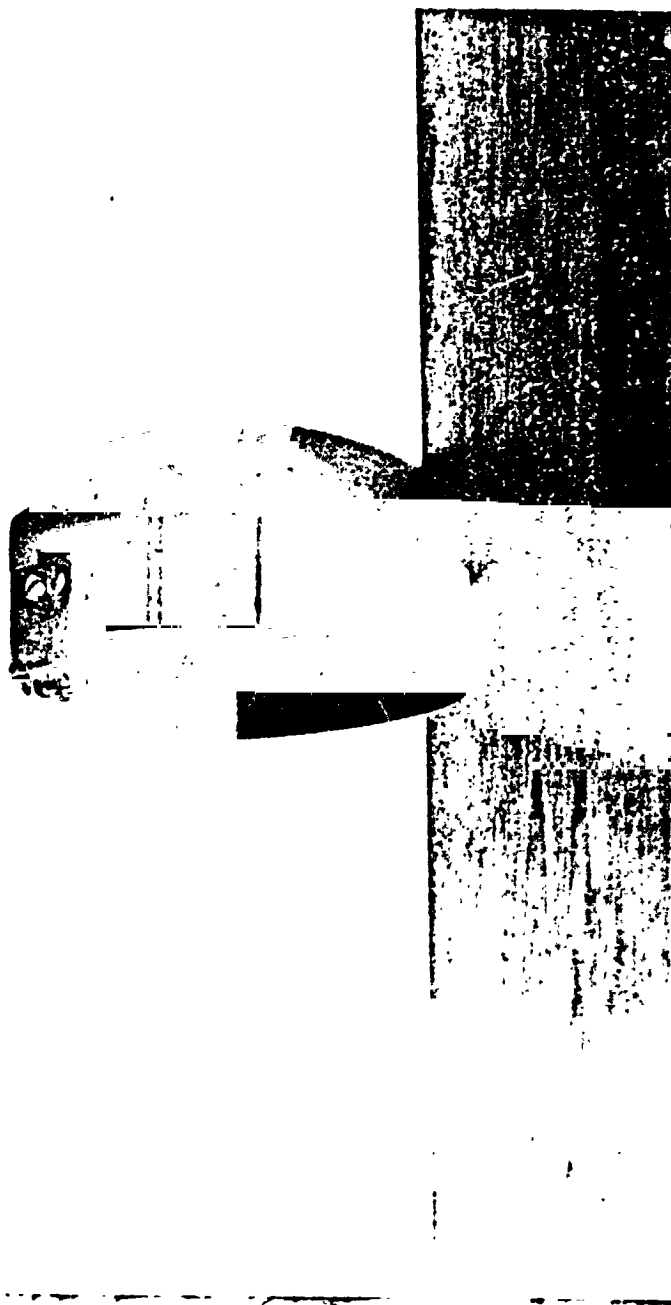


FIGURE 9

OFFSET STANDARD HOOP

rolls away from center, thus tending to stabilize the system. This energy increase, when compared with the decrease upon shifting to the off-center position, is insignificant. The footprint pressure is not reduced by this modification, whereas the problem of stress reversal is magnified. Therefore, this alteration does not lead to a good solution.

If the spoke is mounted to the hoop in the inverted position all of the standard hoop defects are relieved. This system, called the inverted hoop, is shown in Figure 10. The inverted hoop has a configuration such that:

1. Upon compression a very large footprint width is available (Figure 11).
2. There are no inflection points and therefore no stress reversals.
3. When the hoop is forced from the on-center position (Figure 12) there is an internal energy increase which tends to return the hoop to the center position.

The inverted wheel is therefore expected to be far superior to the standard wheel. To assure that this is indeed the case numerous tests were undertaken to compare two full size models. A description of these tests with quantitative results follows in Part 4.

ORIGINAL PAGE IS
OF POOR QUALITY

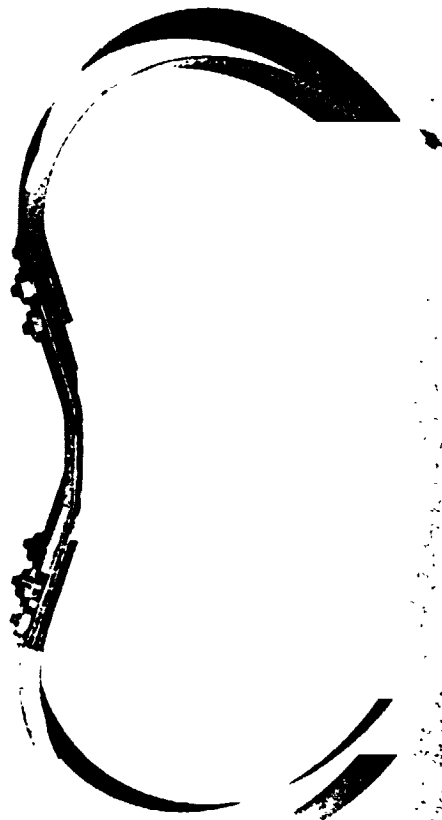


FIGURE 10

INVERTED HOOP - UNLOADED

ORIGINAL PAGE IS
OF POOR QUALITY

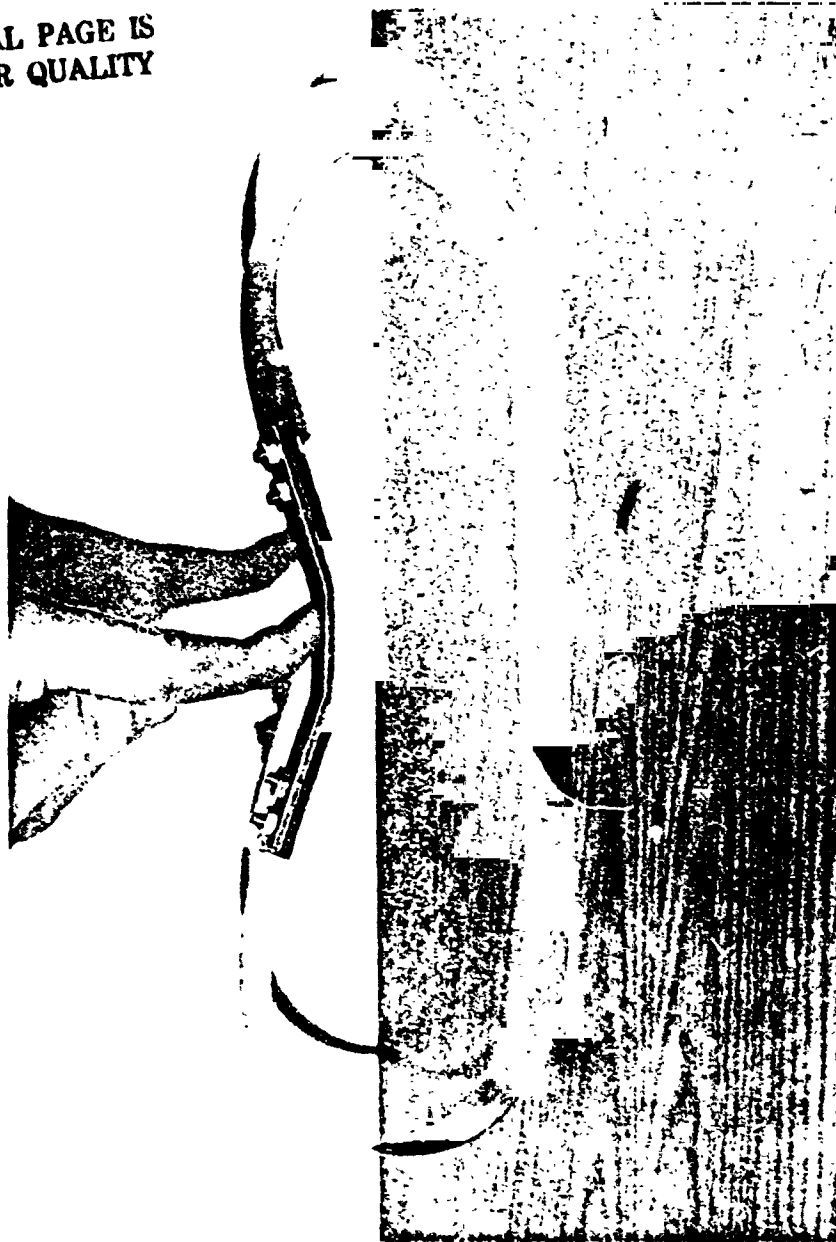


FIGURE 11

INVERTED HOOP - COMPRESSED

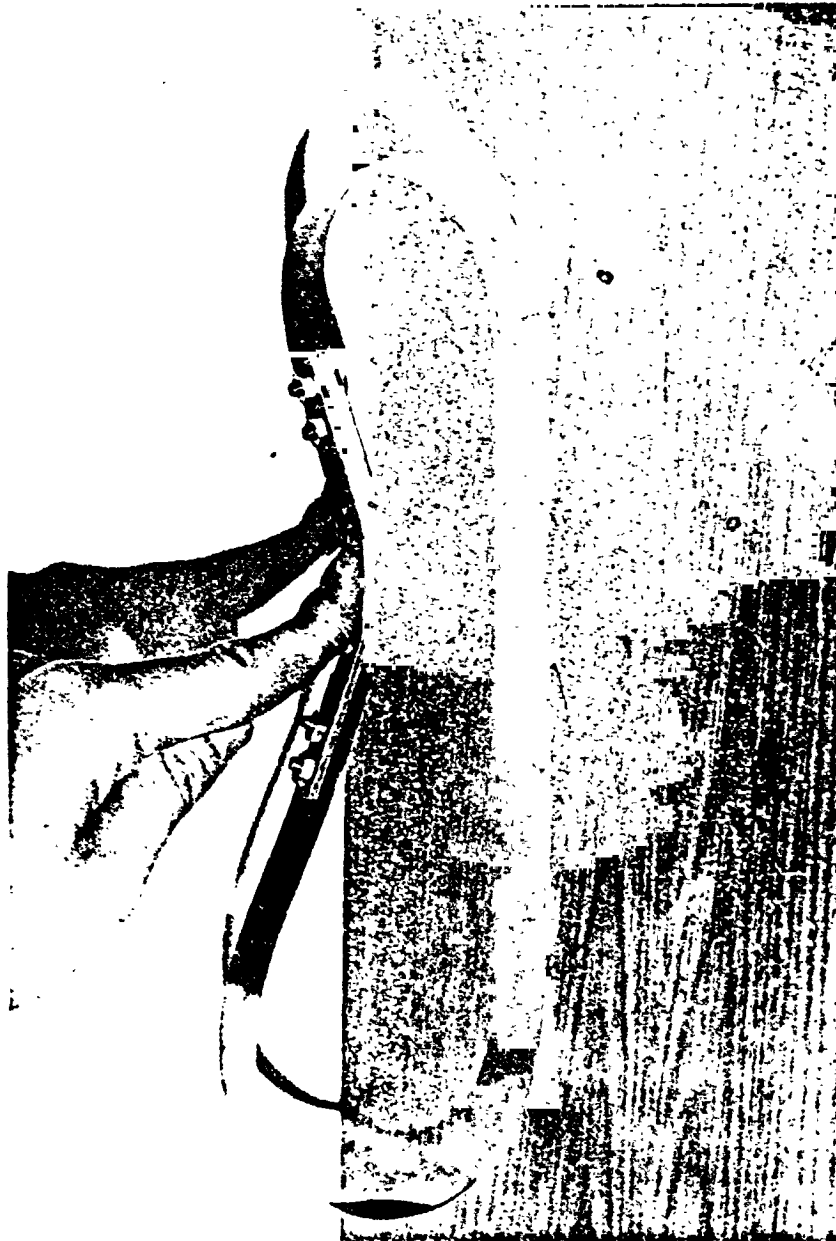


FIGURE 12

INVERTED HOOP - DEFLECTED

PART 4

EXPERIMENTATION

4.1 Inverted versus Standard Toroidal Wheel

Two toroidal wheels of the same parameters were built, one standard and one inverted, and subjected to various tests to assess the value of each. Three experiments were undertaken for each wheel and are described below.

The first comparison was obtained by loading the wheel axle with incrementing weights and the resulting footprint areas were measured. By dividing the normal load by the corresponding area an average pressure is obtained. The results of these experiments are displayed in Figure 13. The inverted wheel is characterized by footprint pressures of one-half to one-sixth that of the standard wheel with footprint areas some two to six times as large. Thus, the inverted wheel is capable of providing the footprint pressures required for a Mars mission.

Subsequent experimentation involved the apparatus shown in Figure 14 to obtain measurements of the net ground thrust as a function of normal axle load. The soil used was dry sand. Weights are applied to the wheel axle and the ground force, N , is measured. An unknown force, Q , is applied to the axle moment arm, r , in the direction of motion. The applied torque, Qr , is equated to the resisting wheel torque, $F R_0$, where F is the net ground thrust and R_0 is the deflected wheel radius under load N . The sum of the forces, $Q + F = F_s$, is measured on a spring scale affixed to the wheel axle. The ground force, F , can then be found

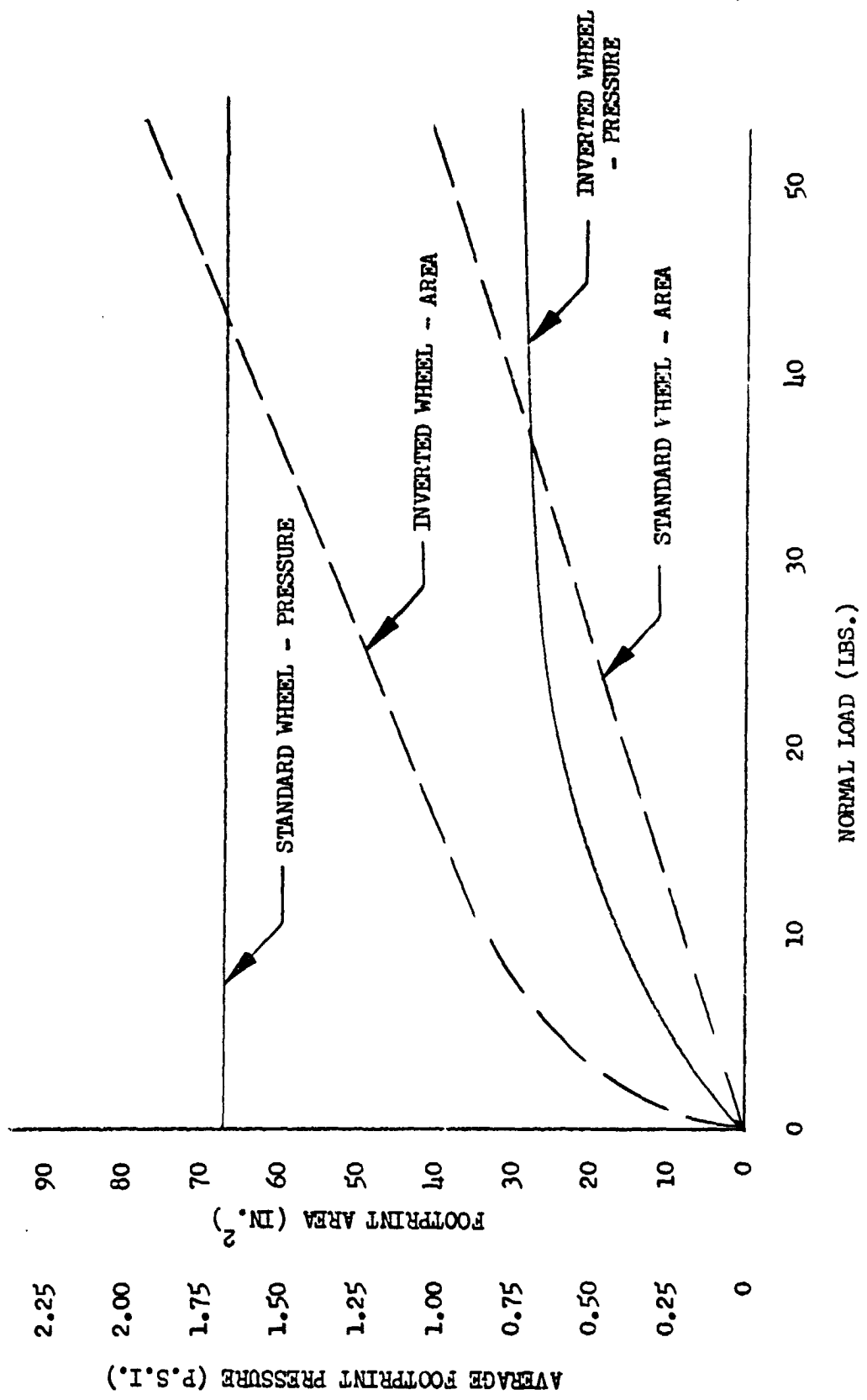


FIGURE 13 LOADING CHARACTERISTICS OF THE STANDARD AND INVERTED WHEELS



FIGURE 11

TRACTION TESTER

as,

$$F = \left(\frac{r}{r + R_o} \right) F_s \quad 4.1.1$$

where,

$$R_o = R_H - \delta \quad 4.1.2$$

which is the unloaded wheel radius less its' loaded deflection. To obtain the deflection as a function of load for each wheel, an Instron tester was used (Figures 15 and 16). The deflection curves are shown in Figure 17. Using these curves and the experimental results, the net ground thrust as a function of load can be correlated for each wheel as shown in Figure 18. At low normal loads there is seen to be only slight thrust differences with the inverted wheel displaying its superiority at higher loads, in which an operating wheel would be expected to perform.

The endurance of each wheel is another important characteristic. The dynamic wheel tester shown in Figures 19 and 20, was used to measure the distance a wheel traveled under operating load until ultimate failure. While the standard wheel ruptured at 2.9 kilometers, the inverted wheel endured 12.9 kilometers with no visible signs of fatigue.

These data suggest that the inverted wheel is by far the superior concept. Any subsequent investigations of the standard toroidal wheel were therefore halted.

4.2 Stress Concentrations

With the total effort now directed towards the inverted wheel, a thorough investigation of any potential problem areas was undertaken. Using the vibration tester, Figure 21, hoops were mounted as shown.

ORIGINAL PAGE IS
OF POOR QUALITY



FIGURE 15

STANDARD WHEEL - DEFLECTION CALIBRATION

ORIGINAL PAGE IS
OF POOR QUALITY

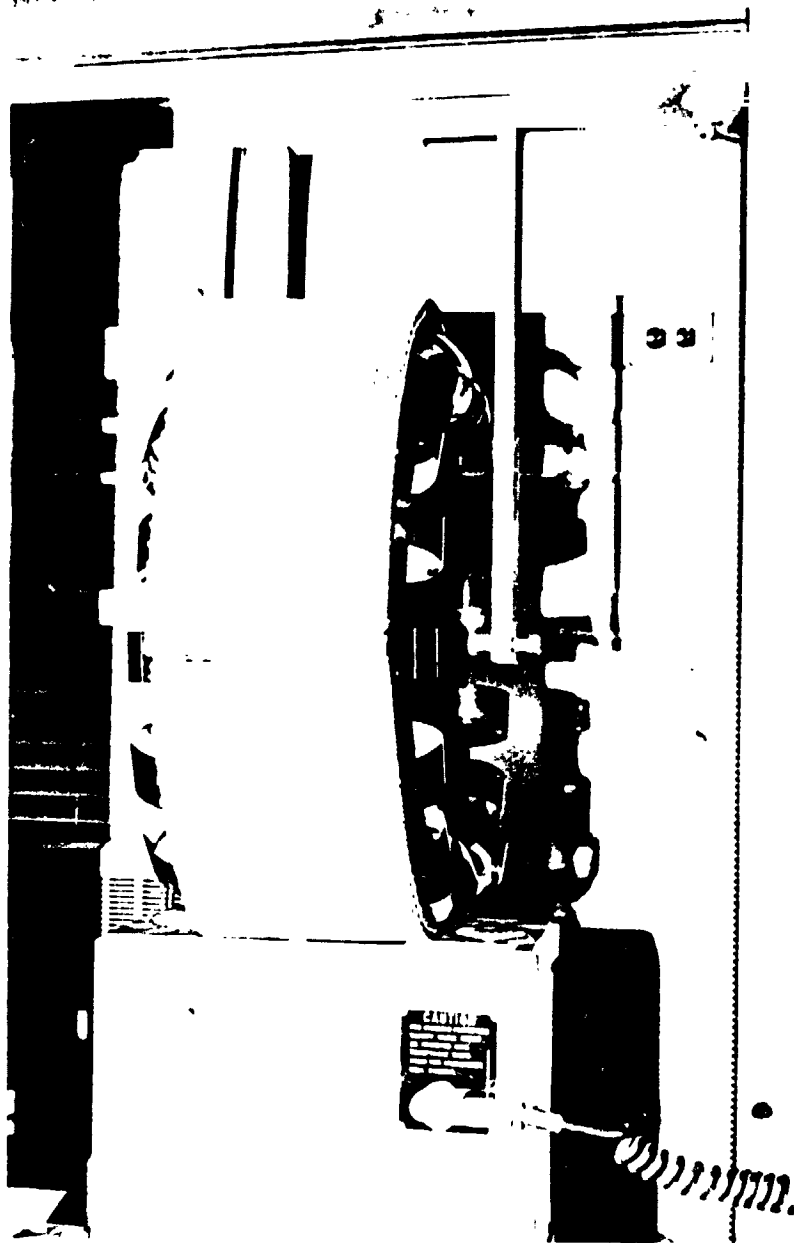


FIGURE 16

INVERTED WHEEL - DEFLECTION CALIBRATION

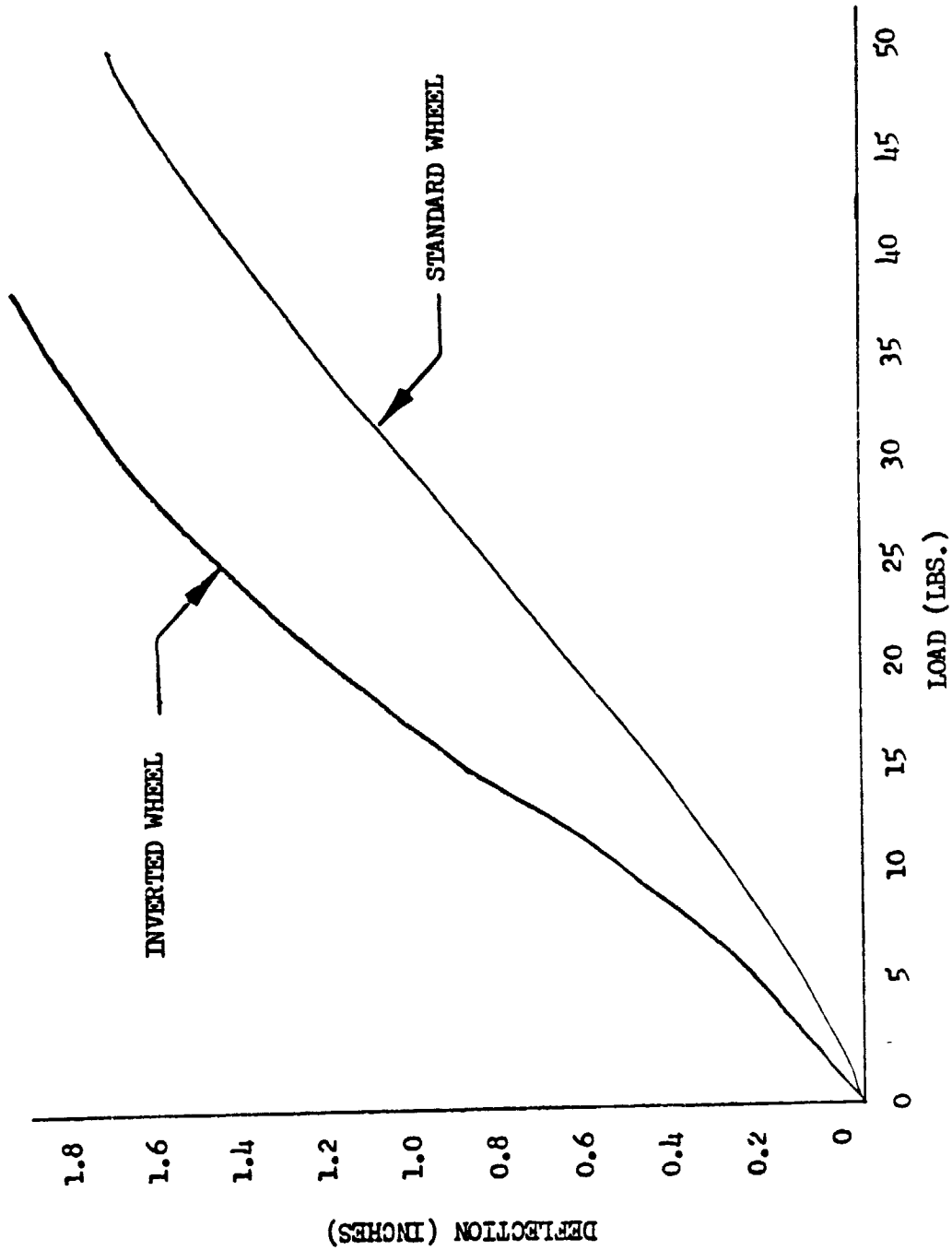


FIGURE 17 DEFLECTION AS A FUNCTION OF LOAD

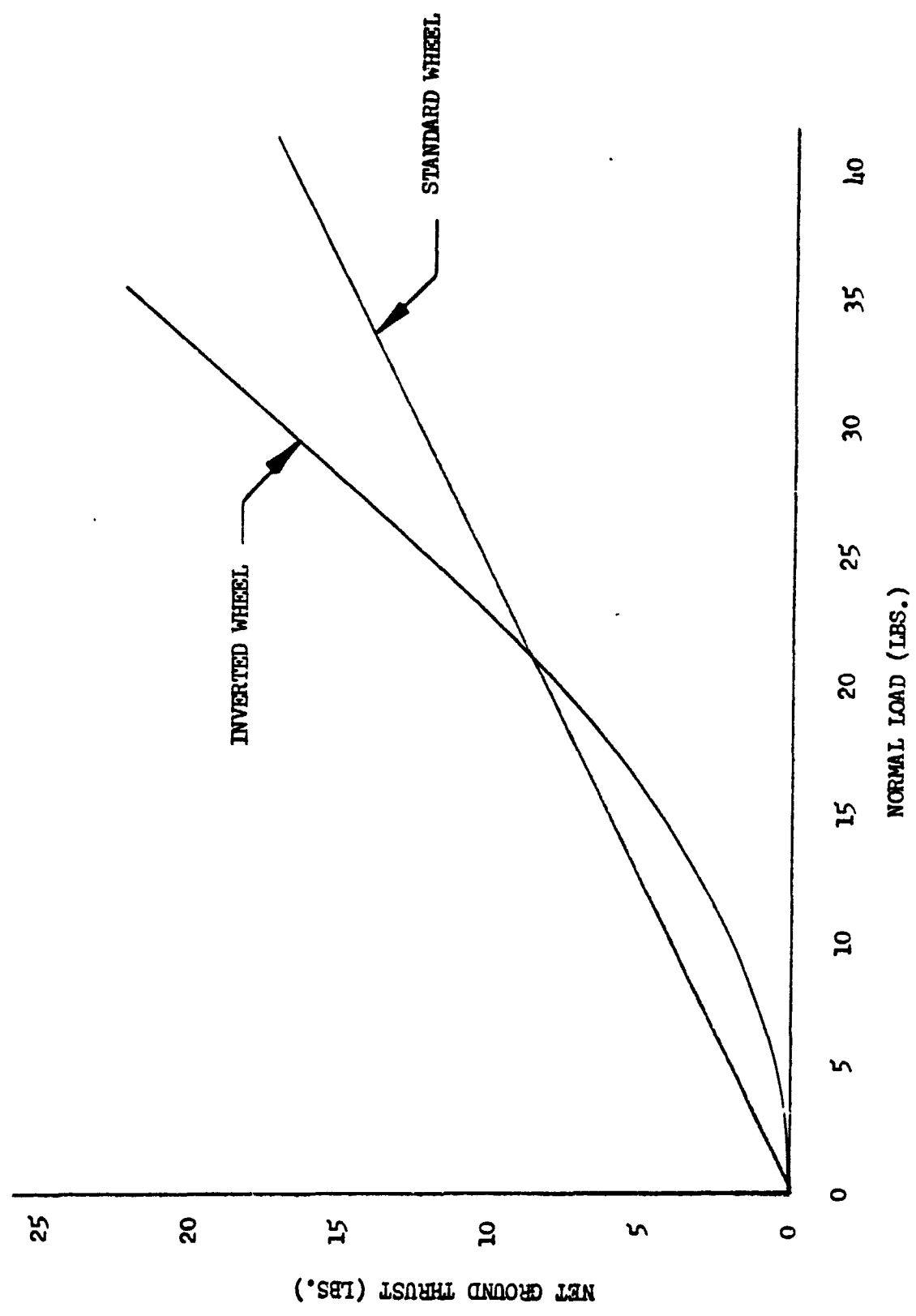


FIGURE 18 NET GROUND THRUST AS A FUNCTION OF LOAD

ORIGINAL PAGE IS
OF POOR QUALITY

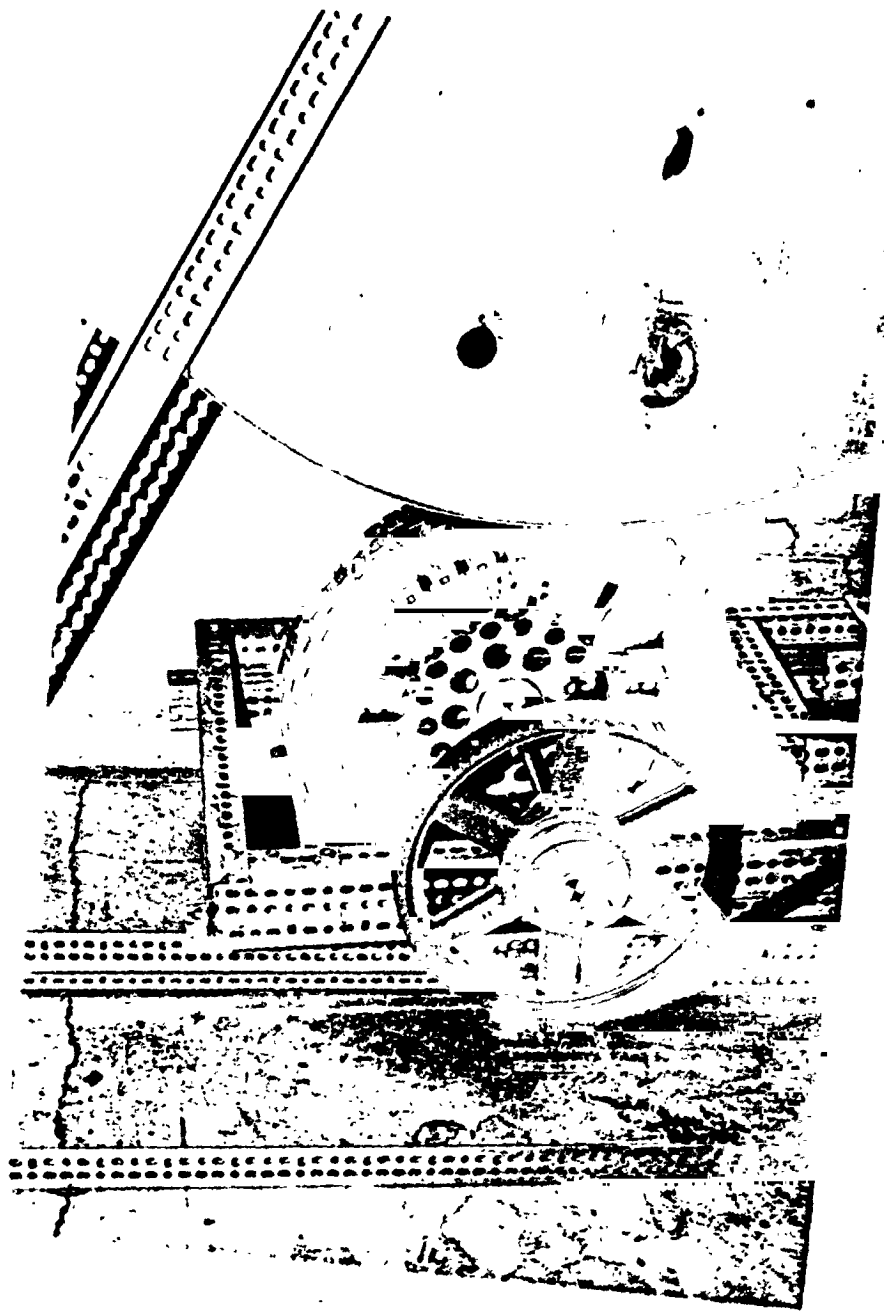


FIGURE 19

STANDARD WHEEL - ENDURANCE TESTING

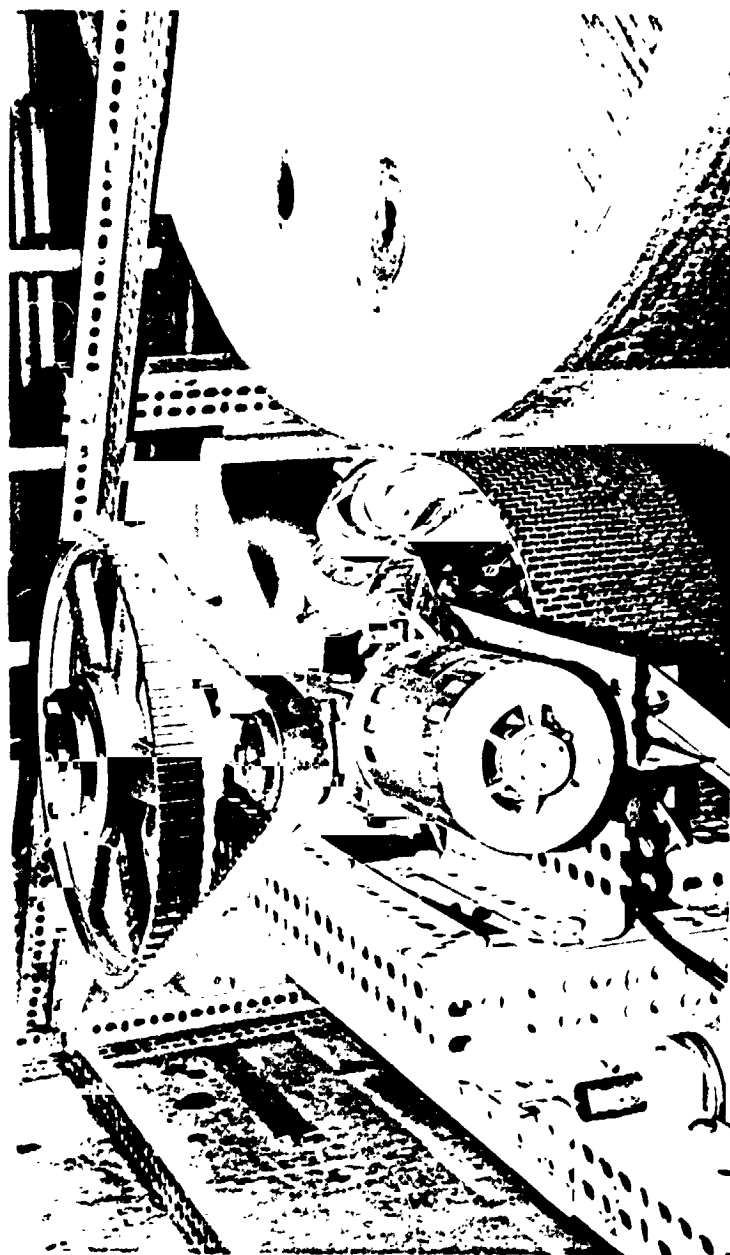


FIGURE 20

INVERTED WHEEL - ENDURANCE TESTING



FIGURE 21

VIBRATION TESTER

Operating at frequencies of 20 hertz one can in effect find where the hoop would fail, after many kilometers of travel, in a very short time. In this manner, the following two stress concentrations have been identified.

An area of very high stress exists where the spoke is joined to the hoop. Failures of the type shown in Figure 22 often occur. Attaching a plate, as displayed in Figure 23, distributes this high stress over the hoop. Vibration tests of three hours and more have not caused any failures when the plate is used.

Conveniently, grousers (tread) have been attached by bolting directly through the hoops. This not only reduces the strength of the hoop, but causes very high stresses in the area of the bolt. Shown in Figure 24 is a new method of attaching grouser. In this manner no material is removed nor are any stress concentrations induced.

ORIGINAL PAGE IS
OF POOR QUALITY



FIGURE 22

HOOP - SPOKE STRESS CONCENTRATION



FIGURE 23

INVERTED HOOP EMPLOYING THE STRESS

DISTRIBUTION PLATE



FIGURE 24

GROUSER ATTACHMENT

PART 5

A MATHEMATICAL MODEL OF THE INVERTED TOROIDAL WHEEL

5.1 Derivation

The design of a wheel to meet special conditions can be approached either from a mathematical or an experimental point of view. Pure experimentation would require an extraordinary amount of data. On the other hand, the complexity of the wheel requires that certain simplifying assumptions be made which must be experimentally verified. A mathematical model has been derived and is described below.

The inverted hoop, being a non-linear spring system, must be quantified about an operating point, from which the solution can be expanded. An operating point does exist and is described by the following statement:

"There is an unknown loading, L_H , which will cause the inverted toroidal hoop-spoke system to assume approximately circular configurations over its outer regions."

This configuration, shown in Figure 25, is called the static condition. Considering this diagram one finds the following geometrical relationships:

The hoop radius of curvature is,

$$R_H = \frac{L/2 - B/2 - S \cos \Theta}{\sin \Theta + \Theta + \pi} \quad 5.1.1$$

The width of the hoop can be found as,

$$W_H = 2(1 + \sin \Theta) R_H + B + 2 S \cos \Theta \quad 5.1.2$$

The clearance between hoop and spoke is:

$$C = (1 + \cos \Theta) R_H - S \sin \Theta \quad 5.1.3$$

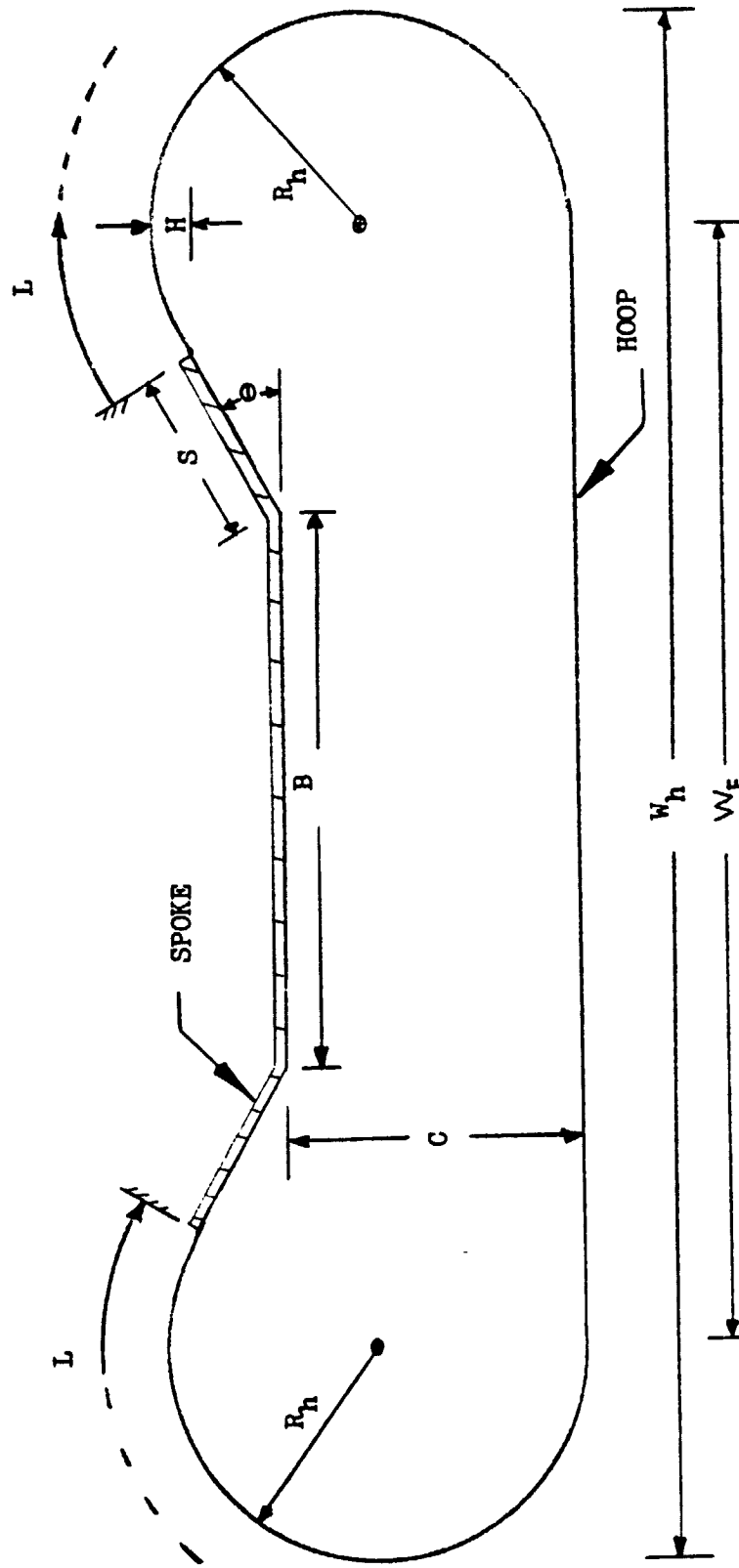


FIGURE 25 STATIC CONDITION

The height is expressed as:

$$H = (1 - \cos \Theta) R_H \quad 5.1.4$$

and the footprint width is found to be:

$$W_F = B + 2(S \cos \Theta + R_H \sin \Theta) \quad 5.1.5$$

Neglecting the shear and axial load variations* at different cross-sections of the circular region of the hoop, a case of pure bending therefore exists. The bending moment is constant and is found from the straight beam flexure formula as:

$$M = \frac{EI}{R_H} \quad 5.1.6$$

where "E" is the material elastic modulus and "I" is the cross-sectional moment of inertia and is computed as:

$$I = 1/12 wt^3 \quad 5.1.7$$

The free body diagrams of Figures 26A and 26B can be used to find the hoop tension, T, and the hoop load, P, as follows. From Figure 26A, the tension is found to be:

$$T = \frac{M}{2 R_H} = \frac{EI}{2 R_H^2} \quad 5.1.8$$

From Figure 26B, the hoop load is expressed as:

$$P = \frac{M}{R_H} - T = \frac{EI}{2 R_H^2} - T \quad 5.1.9$$

Thus the load which produces the static condition is:

$$L_H = 2P = \frac{EI}{R_H^2} \quad 5.1.10$$

* This assumption introduces less than 0.5% error in the majority of cases.

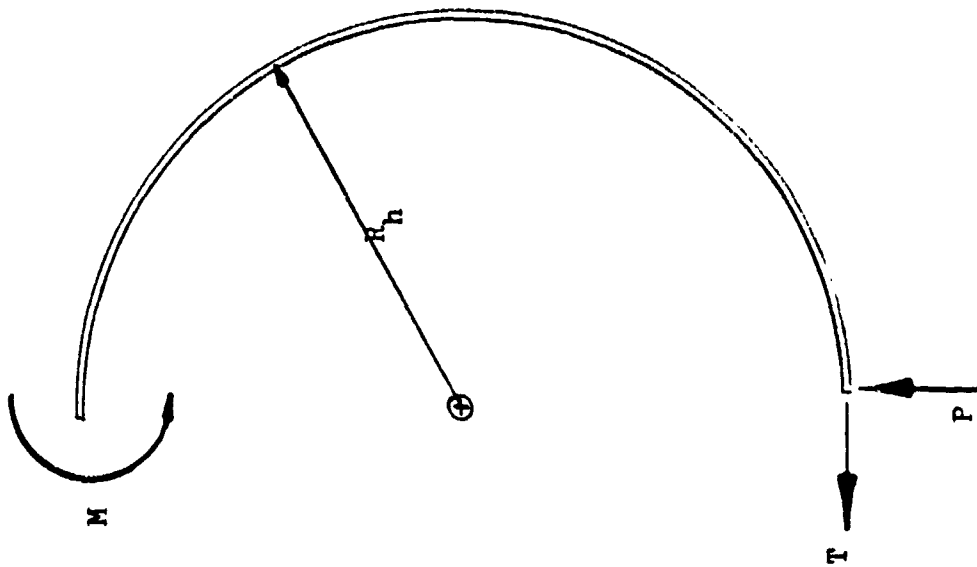


FIGURE 26 A

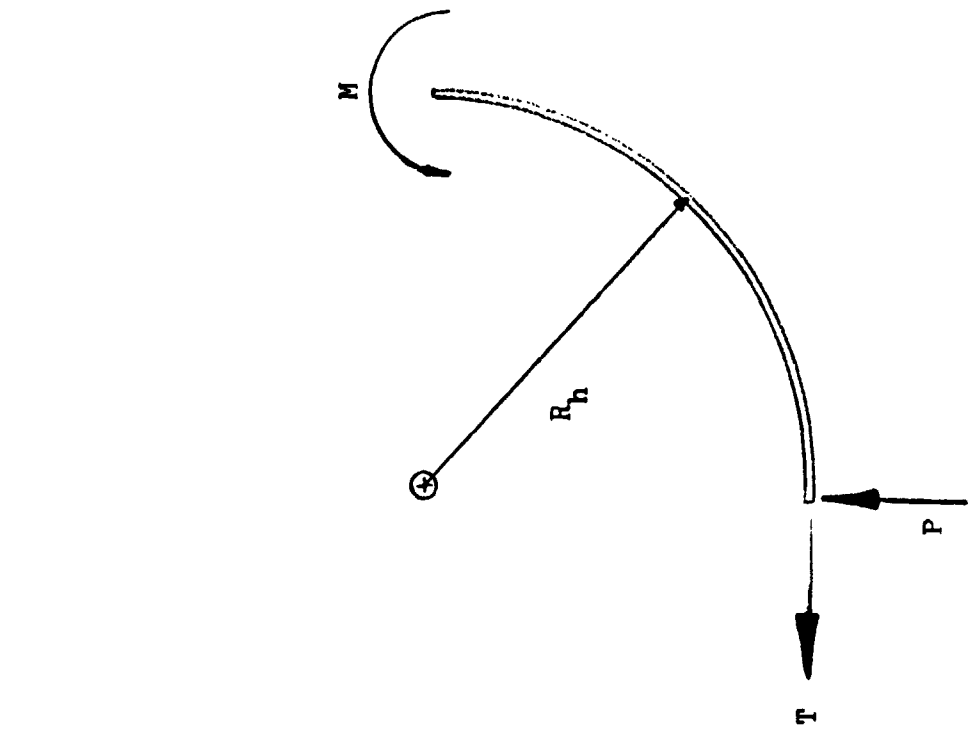


FIGURE 26 B

INVERTED HOOP - FREE BODY DIAGRAMS

If the hoop spring constant at the operating point is assumed not to change as the load L_H , is applied, then this constant can be found from:

$$K = L_H / \delta \quad 5.1.11$$

where " δ " is the deflection caused by application of the load, L_H .

This deflection can be found using Castagliano's Theorem, namely:

"The deflection of a point in an elastic body is equal to the derivative of the strain energy taken with respect to the applied force and is in its direction".

The derivative of the strain energy taken with respect to the load, P , is:

$$\frac{dU}{dP} = \delta = \frac{1}{EI} \int_0^{\pi+\theta} M \frac{dM}{dP} R_H d\phi \quad 5.1.12$$

where " $d\phi$ " is shown in Figure 27. From this diagram an expression for the moment as a function of ϕ is found to be:

$$M = PR_H \sin \phi + TR_H(1 - \cos \phi) \quad 5.1.13$$

but since $T = P$,

$$M = PR_H (\sin \phi - \cos \phi + 1) \quad 5.1.14$$

and from equation 5.1.13:

$$\frac{dM}{dP} = R_H \sin \phi \quad 5.1.15$$

Therefore, combining equations 5.1.12, 14, and 15, the deflection is expressed by:

$$\delta = \frac{1}{EI} \int_0^{\pi+\theta} PR_H^3 \sin \phi (\sin \phi - \cos \phi + 1) d\phi \quad 5.1.16$$

which after integration reduces to:

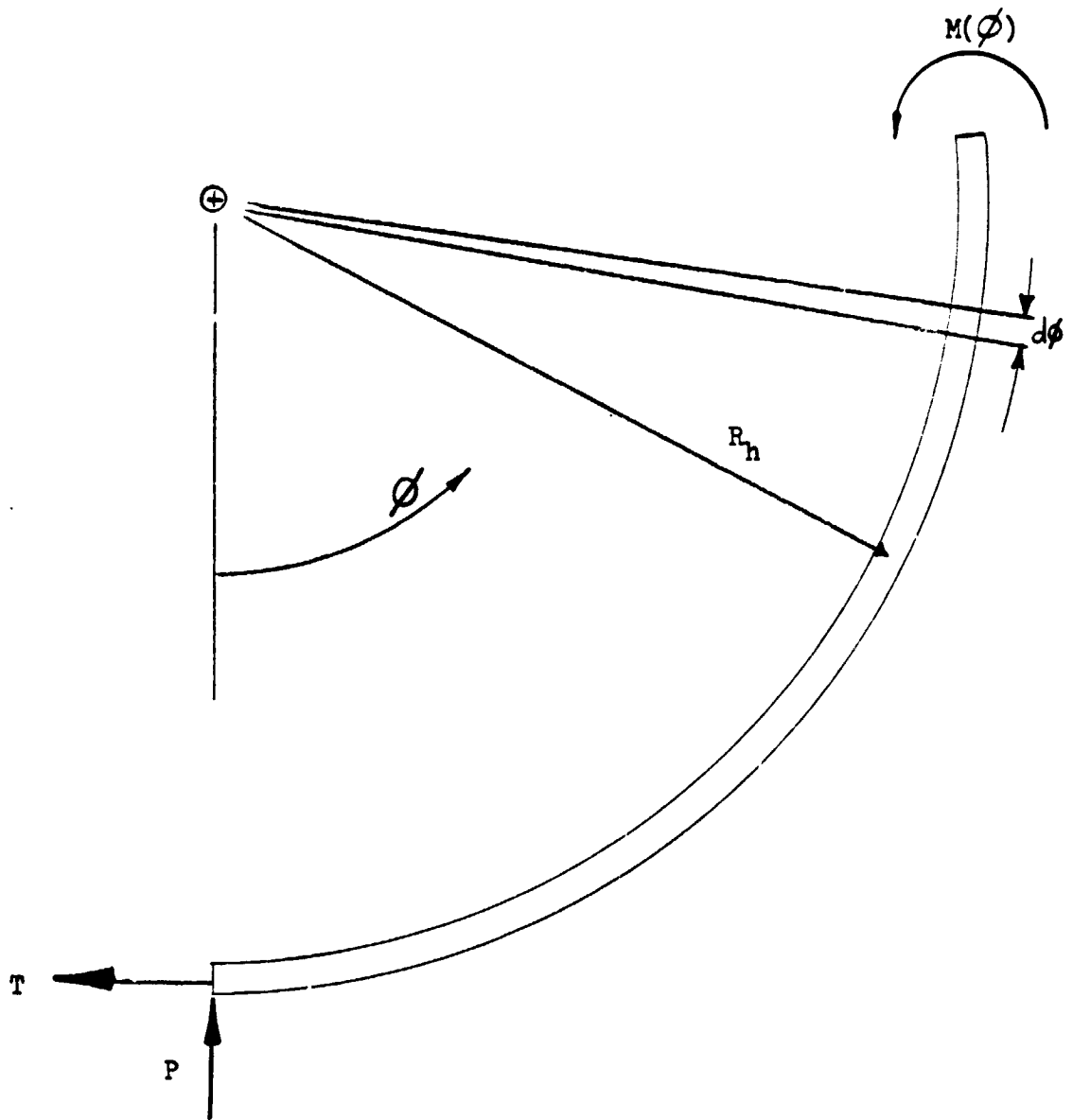


FIGURE 27

INVERTED HOOP - FREE BODY DIAGRAM

$$\delta = \frac{PR^3}{2EI^H} (\pi + \theta - 2 + 2\cos\theta - \sin\theta \cos\theta - \sin^2\theta) \quad 5.1.17$$

Using this equation along with 5.1.10 and 11, the spring constant is expressed as:

$$K = \frac{4EI}{R_H^3} (\pi + \theta - 2 + 2\cos\theta - \sin\theta \cos\theta - \sin^2\theta)^{-1} \quad 5.1.18$$

Figure 28 is a diagram of the inverted wheel under compression.

The footprint area is:

$$A_F = W_F L_F \quad 5.1.19$$

where,

$$L_F = 2\delta \left(\frac{2R_W}{\delta} - 1 \right)^{\frac{1}{2}} \quad 5.1.20$$

where "R_w" is the wheel radius.

Combining equations 5.1.19 and 20 while recalling equation 5.1.5, the footprint area is expressed as:

$$A_F = (B + 2(S \cos\theta + R_H \sin\theta)) (2\delta \left(\frac{2R_W}{\delta} - 1 \right)^{\frac{1}{2}}) \quad 5.1.21$$

To determine the load which is distributed over this area, the contribution from the peripheral hoops must be taken into account. Assuming that all hoops deflect in their own plane, the total axle load can be found as follows:

Letting:

- δ_0 = deflection of the center hoop
- δ_1 = deflection of the first peripheral hoop
- ⋮
- etc.

one obtains:

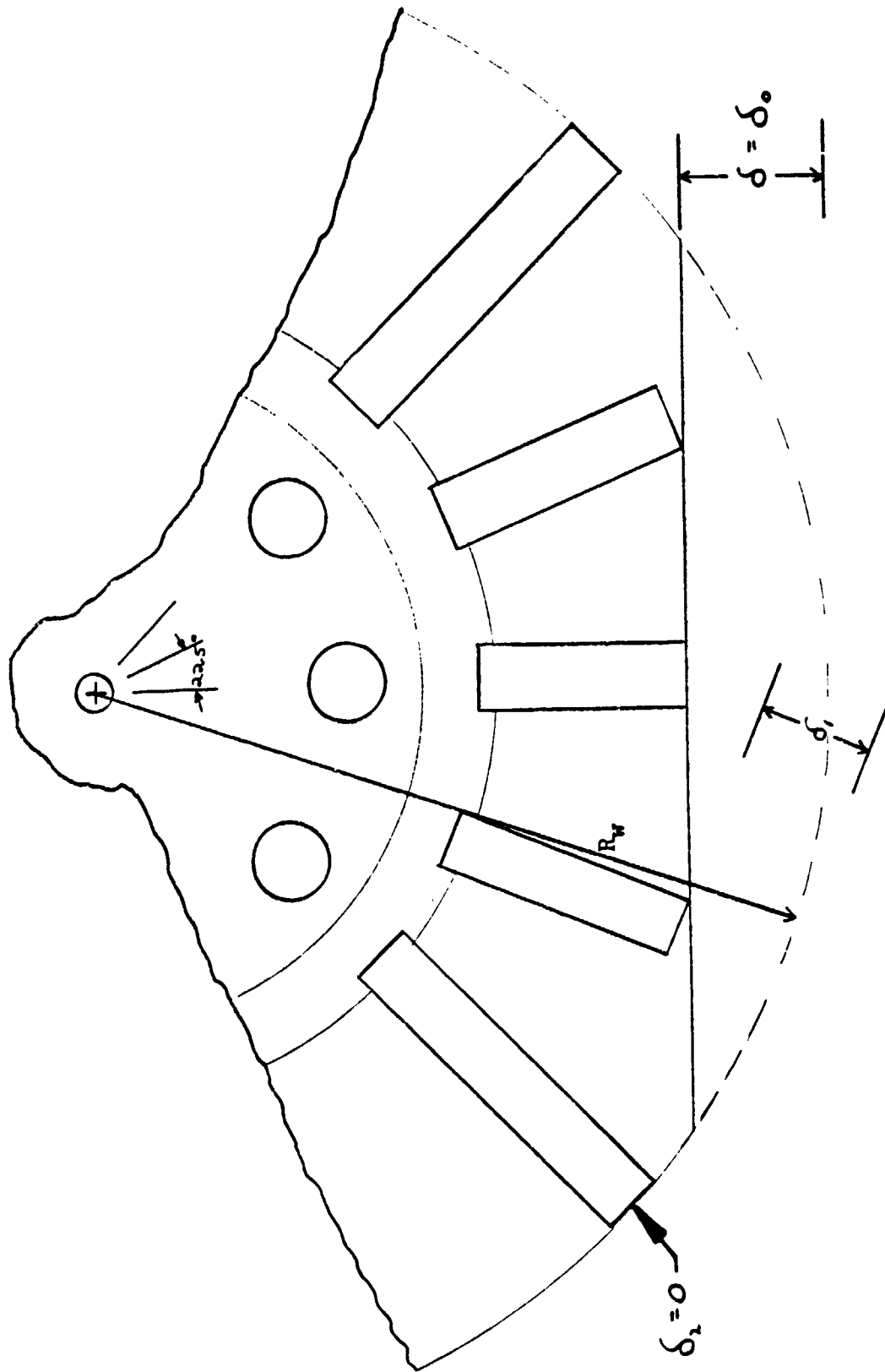


FIGURE 28 INVERTED WHEEL UNDER COMPRESSION

$$\delta_0 = \delta$$

$$\delta_1 = R_W - \frac{R_W - \delta}{\cos 22.5^\circ} = \frac{R_W (\cos 22.5^\circ - 1) + \delta}{\cos 22.5^\circ}$$

$$\delta_2 = \frac{R_W (\cos 45^\circ - 1) + \delta}{\cos 45^\circ}$$

⋮

⋮

etc.

or in general:

$$\delta_N = \frac{R_W (\cos 22.5^\circ N - 1) + \delta}{\cos 22.5^\circ N}$$

5.1.22

Upon compression the peripheral hoops are loaded on their respective angles and therefore contribute only a vertical component to wheel support which is expressed by:

$$F_n = K \delta_N \cos (22.5^\circ N) \quad 5.1.23$$

Combining equations 5.1.22 and 23, one obtains the individual hoop support as:

$$F_N = K \left[R_W (\cos (22.5^\circ N) - 1) + \delta \right] \quad 5.1.24$$

Summing this expression over the hoops in ground contact yields the expression for the wheel support as:

$$L_W = \left\{ 2 \sum_1^N \left[(\cos 22.5^\circ N - 1) R_W + \delta \right] + \delta \right\} K \quad 5.1.25$$

The average pressure is then found as:

$$P_a = L_W / A_F \quad 5.1.26$$

Since the wheel support will not, in general, be equal to the axle load imposed, one must superimpose a number of hoop bands to equate the forces. The number of bands, B_N , required can be found from:

$$B_N = \frac{L_A + W_W}{L_W} \quad 5.1.27$$

where " L_A " is the axle load, and " w " is the wheel weight. The inverted wheel, less hoops, weighs approximately five pounds. The weight of the hoops can be found as:

$$16 (\rho t w L) B_N$$

thus,

$$B_N = \frac{L_A + (5 + 16\rho t w L B_N)}{L_W} \quad 5.1.28$$

solving for B_N yields:

$$B_N = \frac{L_A + 5}{L_W - 16\rho t w L} \quad 5.1.29$$

A multiple band hoop is shown in Figure 29.

5.2 Computer Programs

The preceding derivation does not allow one to synthesize the desired wheel characteristics. Rather, it transforms the chosen input into the corresponding output. Using the "Inverted Toroidal Wheel Program" listed in Appendix A, a search is carried out by incrementing the input parameters of hoop length, spoke base length, spoke flange length, and spoke flange angle. The material, its properties, the axle load and overall wheel radius are also provided as input. To limit the number of solutions, only wheels satisfying a chosen safety factor and wheel weight are printed. Other outputs to consider before a wheel is accepted as a solution will be discussed in Part 6. Table 1 shows a partial sample printout.

Once the number of bands is found from the program output, one needs to know the length to which each should be manufactured such that no hoops

ORIGINAL PAGE IS
OF POOR QUALITY



FIGURE 29

MULTIPLE BAND INVERTED HOOP

MATERIAL: SPRING STEEL - 0.95% C

HOOP THICKNESS = 0.015 HOOP WIDTH = 1.00

YOUNG'S MODULUS = 0.30E 08 YIELD STRESS = 0.18E 06

DESIGN LOAD = 40.0

HOOP DENSITY = 0.284

YIELD POINT RADIUS = 1.25

WHEEL RADIUS = 10.00

HOOP CRITERIA : SF = 1.20 , WW = 20.0

TABLE 1

INVERTED TOROIDAL WHEEL PROGRAM -
SAMPLE OUTPUT

#	L	B	S	TH	RH	SF	WH	C	CO	H	LH	LW	BN	HW	LF	WF	AF	PA
12	18.0	1.0	2.0	20.0	1.7	1.38	9.4	2.7	3.9	0.10	2.8	5.1	11.7	19.3	9.7	5.7	57.9	1.025
13	18.0	1.0	2.0	30.0	1.6	1.30	9.3	2.0	3.1	0.22	3.2	5.2	11.4	19.0	9.1	6.1	55.6	1.061
14	18.0	1.0	2.0	40.0	1.6	1.24	9.2	1.5	2.4	0.36	3.5	4.9	12.2	19.9	8.5	6.1	51.4	1.157
16	18.0	1.0	2.5	10.0	1.7	1.38	10.0	3.0	4.3	0.03	2.8	5.2	11.2	18.8	10.0	6.5	65.1	0.902
17	18.0	1.0	2.5	20.0	1.6	1.28	10.0	2.3	3.4	0.10	3.3	5.6	10.3	17.7	9.4	6.8	64.0	0.902
18	18.0	1.0	2.5	30.0	1.5	1.22	9.9	1.6	2.6	0.20	3.6	5.6	10.4	17.7	8.8	6.9	60.6	0.952
21	18.0	1.0	3.0	10.0	1.6	1.27	10.6	2.6	3.9	0.02	3.3	5.9	9.7	16.9	9.6	7.9	71.6	0.795
32	18.0	2.0	1.5	20.0	1.7	1.32	9.4	2.8	4.1	0.10	2.9	5.1	11.6	19.2	9.7	6.0	58.3	1.016
33	18.0	2.0	1.5	30.0	1.6	1.29	9.4	2.3	3.3	0.22	3.3	5.2	11.2	18.8	9.1	6.2	56.4	1.042
34	18.0	2.0	1.5	40.0	1.5	1.22	9.3	1.7	2.7	0.36	3.6	5.0	11.9	19.6	8.5	6.1	53.1	1.123
36	18.0	2.0	2.0	10.0	1.7	1.38	10.0	3.1	4.4	0.03	2.8	5.2	11.2	18.7	10.0	6.5	65.2	0.900
37	18.0	2.0	2.0	20.0	1.6	1.28	10.0	2.4	3.6	0.10	3.3	5.6	10.2	17.6	9.4	6.9	64.3	0.895

TABLE 1 (CONT.)

ORIGINAL PAGE IS
OF POOR QUALITY

are in contact over the circular area of the hoop band. The reason for this is that when an inner hoop compresses, its outer surface expands, while the inner surface of the outer adjacent hoop contracts. This type of shearing effect would change the systems character from that which is expected. Appendix B lists the "Bands Program" which yields the interference lengths as well as the manufacturing lengths for each hoop of a multiband system. Table 2 is a sample printout for a 10 band inverted hoop.

5.3 Verification of the Inverted Toroidal Wheel Derivation

Various hoops, whose parameters were taken from computer output, were built and experimentally verified. Table 3 shows that the experimental quantities agree very well with the theoretical predictions. An extremely important correlation is that of the deflection values. This shows that the linear spring assumption is indeed valid, and that the summation technique, used to go from a hoop to a wheel, might be a good approximation.

To further validate the summation techniques, an inverted wheel was built and tested. Table 4 compares the experimental and theoretical inverted wheel.

DESIGN LENGTH = 24.0

BASE LENGTH = 3.0

FLANGE LENGTH = 1.0

FLANGE ANGLE = 30.0

THICKNESS = 0.018

NUMBER OF BANDS = 10

ORIGINAL PAGE IS
OF POOR QUALITYBAND NUMBER = 1
LENGTH = 23.33LENGTH CHANGE = -0.67
MANUFACTURING LENGTH = 21.98BAND NUMBER = 2
LENGTH = 23.48LENGTH CHANGE = -0.52
MANUFACTURING LENGTH = 22.43BAND NUMBER = 3
LENGTH = 23.63LENGTH CHANGE = -0.37
MANUFACTURING LENGTH = 22.88BAND NUMBER = 4
LENGTH = 23.78LENGTH CHANGE = -0.22
MANUFACTURING LENGTH = 23.33BAND NUMBER = 5
LENGTH = 23.93LENGTH CHANGE = -0.07
MANUFACTURING LENGTH = 23.73BAND NUMBER = 6
LENGTH = 24.07LENGTH CHANGE = 0.07
MANUFACTURING LENGTH = 24.22BAND NUMBER = 7
LENGTH = 24.22LENGTH CHANGE = 0.22
MANUFACTURING LENGTH = 24.67BAND NUMBER = 8
LENGTH = 24.37LENGTH CHANGE = 0.37
MANUFACTURING LENGTH = 25.12BAND NUMBER = 9
LENGTH = 24.52LENGTH CHANGE = 0.52
MANUFACTURING LENGTH = 25.57BAND NUMBER = 10
LENGTH = 24.67LENGTH CHANGE = 0.67
MANUFACTURING LENGTH = 26.02TABLE 2BANDS PROGRAM - SAMPLE OUTPUT

HOOP NO.	L	B	S	Θ	C _o	C	W _h	H	R _h	W _f	L _h
43	16	1	1.5	20	3.9	2.9	8.1	0.1	1.6	5.0	4.0 *
					3.7	2.6	8.1	0.2	1.6	4.9	4.2 **
163	18	1	1.0	20	4.6	3.7	8.2	0.1	1.9	3.5	2.3 *
					4.9	3.5	8.2	0.1	1.9	4.2	2.7 **
224	18	3	2.0	40	2.9	1.5	10.1	0.7	1.6	6.0	1.8 *
					2.5	1.6	10.6	0.6	1.4	7.9	5.5 **
293	20	1	1.5	20	5.0	3.8	9.6	0.3	2.1	4.8	2.3 *
					5.1	3.6	9.5	0.3	2.1	5.3	2.3 **
350	20	3	2.0	40	3.5	2.2	11.0	0.9	1.7	7.1	2.4 *
					2.4	1.5	11.2	0.9	1.6	8.1	4.4 **
362	20	4	1.0	10	5.3	4.6	10.5	0.0	2.2	4.5	1.9 *
					5.4	3.8	10.7	0.0	2.0	6.7	2.6 **
438	22	2	1.0	20	5.6	4.5	10.2	0.2	2.3	4.0	1.7 *
					5.0	4.2	10.2	0.2	2.4	5.5	1.8 **
487	22	4	1.0	10	6.0	4.5	11.5	0.1	2.3	6.0	2.4 *
					6.2	4.4	11.4	0.1	2.3	6.8	2.0 **
538	24	1	1.0	20	6.3	4.7	10.6	0.4	2.5	4.7	1.8 *
					7.0	5.0	10.3	0.3	2.8	4.8	1.4 **

* EXPERIMENTAL DATA

** COMPUTER OUTPUT

TABLE 3 THEORETICAL VS. EXPERIMENTAL HOOPS

	<u>EXPERIMENTAL WHEEL</u>	<u>THEORETICAL WHEEL</u>
L =	16.5 in.	16.5 in.
B =	2.5 in.	2.5 in.
S =	1.0 in.	1.0 in.
θ =	45.0 deg.	45.0 deg.
L_w =	5.70 lbs.	5.75 lbs.
L_f =	7.5 in.	7.8 in.
W_f =	5.7 in.	5.8 in.
A_f =	42.75 in. ²	45.20 in. ²
P_a =	0.133 p.s.i.	0.127 p.s.i.

TABLE 1THEORETICAL VS. EXPERIMENTAL WHEEL

PART 6

WHEEL CRITERIA

6.1 Output Characteristics

The design of a wheel requires one to decide on limits for the calculated output characteristics. Any wheel which satisfies all criteria is therefore acceptable and from this group one must weigh the pros and cons of each to determine the best wheel for its proposed purpose. The characteristics which must be considered are:

1. Efficiency
2. Safety Factor
3. Footprint Pressure
4. Lateral Stability
5. Clearances
6. Band Number

The efficiency of the inverted wheel system is defined as the weight that the wheel will support per unit weight of wheel. For a successful mobility system this ratio must be as high as possible, thus allowing more vehicle weight to be in the desired form of instrumentation.

The safety factor, η , is defined as the ratio of the yield point bending moment to the bending moment produced by the static condition. Thus, if η is greater than one, a wheel can then suffer an amount of dynamic load without yielding. The safety factor, η , is rather misleading. The reason for this is that at zero load, a bending moment already exists. Thus, upon application of load, L_w , the bending moment changes by an amount $M_{L_w} - M_o$ or ΔM . If the bending moment is assumed to change linearly with the applied axle load, then one can see that a safety factor, η , as small as 1.2 can allow for axle loads to be multiplied by a much higher factor before yielding occurs. A typical η of 1.2 will allow for the yield point axle load to be approximately double that of the static

condition axle load. This value was therefore adopted for a minimum.

The proposed Mar's rover mission will involve a vehicle of approximately 1500 earth pounds. This translates to 140 pounds per wheel on the Martian surface. Thus, a footprint area of 140 square inches minimum to 280 square inches maximum would be acceptable.

A measure of hoop lateral stability is the vertical distance, H , that the hoop extends above the hoop-spoke interface. The explanation of this lies in the fact that large H values lead to a greater change in stored energy upon lateral deflection. Experiments have shown that a minimum stability is obtained with a value of 0.1 inches.

The static clearance, C , must be compared to the deflection, δ , to assure sufficient clearance from "bottoming out" during shock or dynamic loads. If the hoop spring constant, K , is assumed to be constant through all deflections, then to allow for a dynamic load equal to that of the static load, a static clearance, C , equal to δ must be available. Thus, for a minimum, the no-load clearance, C_0 , must be at least twice that of the static load, C .

Due to manufacturing difficulties and to the possibility of soil clogging, wear, and shear friction, the best solution is the one band wheel. No minimum will be chosen, but all factors being equal, the superior wheel will require the lowest number of bands.

6.2 Wheel Life

The life of any mechanical system is defined as the number of cycles of stress fluctuation the system will endure before rupture occurs. The phenomenon of fatigue failure is very complex and has yet to be theoretically quantified. Therefore, much experimental data exists in the literature

and from this various methods have been contrived to estimate the fatigue life of a mechanical component. Experiments with steel, when plotted on semi-log axes will yield a linear minimum life line. The end points of this line, as shown in Figure 30, are σ_u at 10^3 cycles and $0.5 \sigma_u$ at 10^6 cycles, where σ_u is the materials ultimate strength. Beyond 10^6 cycles the curve is horizontal suggesting infinite life. This curve, referred to as an S-N diagram (stress-number of cycles), is valid for complete stress reversal only. In the case of the inverted toroidal wheel, an alternating stress superimposed on a mean stress is seen to exist as the wheel traverses a terrain. To transform this stress state into the required state of complete stress reversal one can use the Goodman diagram. This diagram, shown in Figure 31, is a cartesian plot with the mean stress, σ_m , along the x-axis and the alternating stress, σ_a , along the y-axis. The infinite life line is defined as a linear curve through the points $0.5 \sigma_u$ and the yield point stress, σ_{yp} , as shown. Drawing a parallel line through the point defined by (σ_m, σ_a) , to the infinite life line will yield the equivalent completely reversed stress as the y-intercept. One then determines the expected life from the S-N diagram.

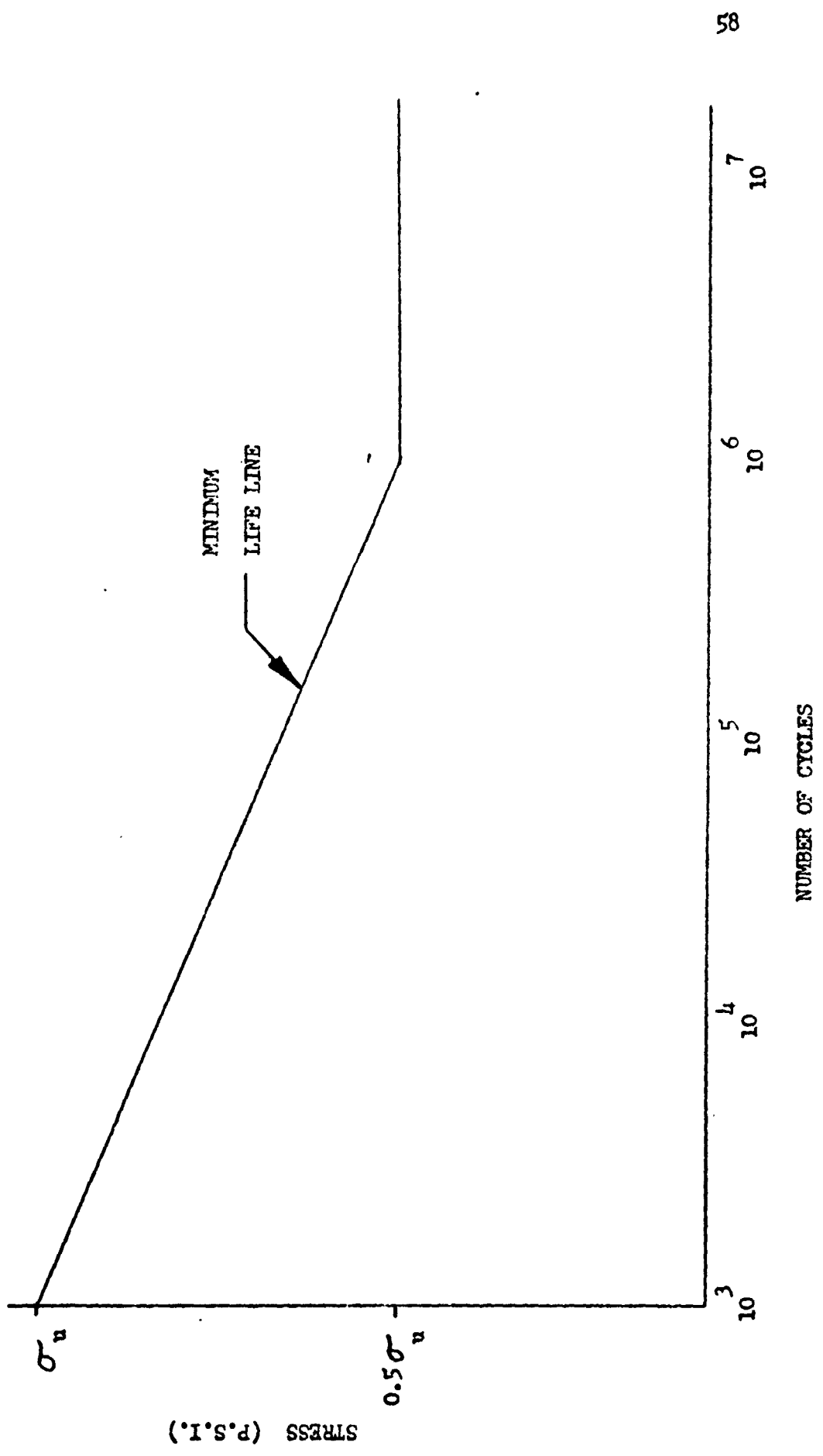
Although this technique is very imprecise, an inverted wheel was built and determined by this method to rupture at approximately 40,000 cycles. Using the dynamic wheel tester, this wheel was experimentally ruptured at 42,600 cycles. Thus, taking into account the many assumptions of the preceding technique, an additional confirmation of the inverted toroidal wheel derivation is evidenced.

6.3 Wheels for the RPI Proto-Type vs. Wheels for a Mar's Mission

The wheels desired for the RPI Rover are to be in the infinite life

FIGURE 30

S - N DIAGRAM FOR STEEL



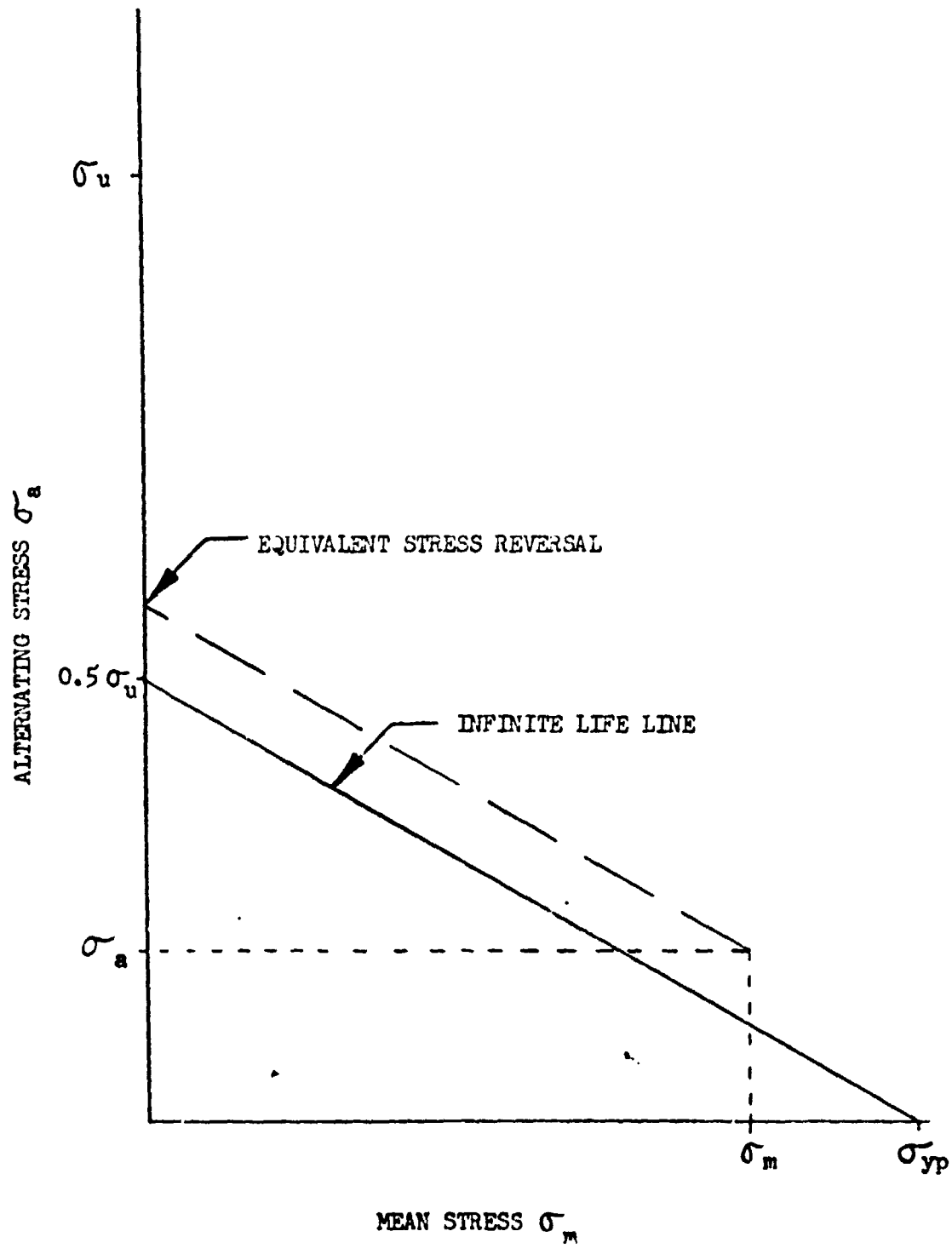


FIGURE 31

GOODMAN DIAGRAM

group, i.e. $\sigma_{a_{max}} \leq 0.5 \sigma_u$. The reason for this is because of the nature of the vehicle, in that it has no limited mission. In contrast, for a Mar's mission finite life wheels, which will inherently weigh much less, may be acceptable. For example, the proposed mission of 100 kilometers would do very well with 200 kilometer wheels at a profitable savings in weight. Thus, before a particular wheel is approved it must meet minimum life specifications. As a general rule it is found that when the safety factor is equal to one, the wheel is marginally infinite, i.e. a minimum life of 10^6 cycles is expected. Of course, dynamic loads will reduce the expected life. This may be included as a random stress requiring a more sophisticated technique, or by simply requiring the wheel life to be some multiple of the proposed mission length thereby providing a margin of safety.

PART 7

COMPUTER OUTPUT

7.1 Wheels for the RPI-Mars Roving Vehicle

The synthesis of an inverted wheel for any rover requires that the investigator choose input parameters which would seem to be compatible with the vehicle. The RPI-Mars roving vehicle, as shown in Figure 32, weighs 160 pounds stripped of its standard wheels. This half scale model is approximately six feet long, four feet wide, and two feet high. Thus, the search for an inverted wheel for this vehicle requires that the axle load be 40 pounds. The wheel radius was chosen as 10 inches. The hoop width was set to 1 inch so that the solutions are "per inch". Numerous combinations of hoop length, base length, flange lengths, and flange angle were tried with the best solutions found in the following ranges:

Hoop Length, L =	18.0 to 26.0 inches
Base Length, B =	1.0 to 5.0 inches
Flange Length, S =	1.0 to 3.0 inches
Flange Angle, Θ =	10° to 50°

For each material employed, the optimum thickness was determined by trial and error. Table 5 is a partial printout for 0.018 inch spring steel - 0.95% carbon. Although this material is one of the superior grades of steel, an acceptable solution cannot be obtained since the band numbers are not close to 1.0 and the maximum efficiency is only 2.7. Beta Titanium, whose partial output is shown in Table 6, has an optimum thickness of 0.028. Although the efficiencies are above four, and the band numbers are down to three, this wheel is still not acceptable. Turning to composites, S-Glass/Epoxy, which is listed in Table 7, shows very

ORIGINAL PAGE IS
OF POOR QUALITY

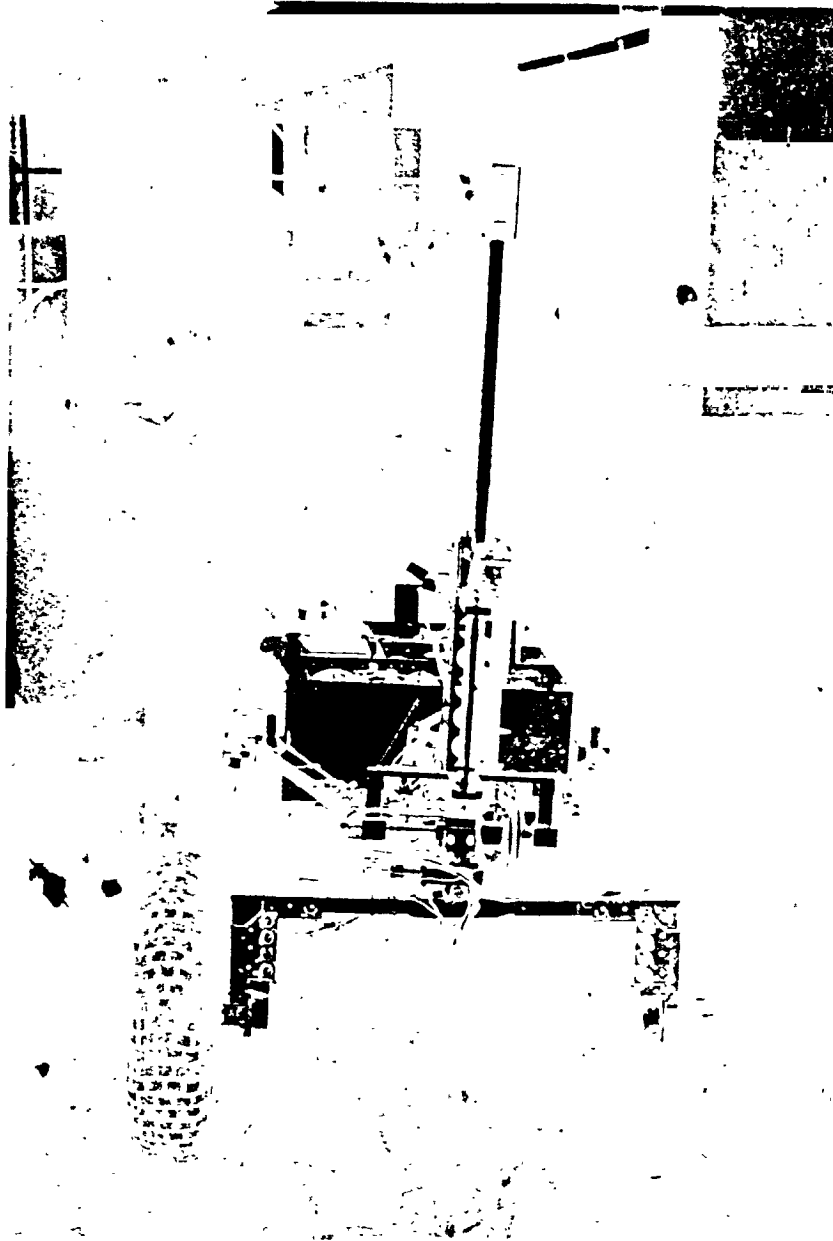


FIGURE 32

R.P.I. MARS ROVING VEHICLE

MATERIAL: SPRING STEEL - 0.95% C

HOOP THICKNESS = 0.018 HOOP WIDTH = 1.00

YOUNG'S MODULUS = 0.30E 08 YIELD STRESS = 0.18E 06

DESIGN LOAD = 40.0

HOOP DENSITY = 0.284

YIELD POINT RADIUS = 1.50

WHEEL RADIUS = 10.00

HOOP CRITERIA : SF = 1.20 . WW = 20.0

TABLE 5 WHEELS FOR THE RPI ROVER - STEEL

#	L	B	S	TH	RH	SF	MH	C	CO	H	LH	LW	BN	WW	LF	WF	AF	PA
1	18.0	1.0	1.0	10.0	2.2	1.44	8.0	4.1	5.8	0.03	3.1	6.5	8.9	18.0	11.0	3.7	41.0	1.415
2	18.0	1.0	1.0	20.0	2.0	1.32	8.2	3.5	4.9	0.12	3.7	7.3	7.7	16.4	10.4	4.2	43.8	1.287
3	18.0	1.0	1.0	30.0	1.8	1.22	8.2	2.7	4.2	0.25	4.3	7.7	7.2	15.6	9.7	4.0	44.1	1.261
6	18.0	1.0	1.5	10.0	2.0	1.34	8.7	3.7	5.3	0.03	3.6	7.1	7.8	16.4	10.7	4.7	49.8	1.133
7	18.0	1.0	1.5	20.0	1.9	1.23	8.8	3.1	4.4	0.11	4.3	8.0	6.9	15.2	10.1	5.1	51.1	1.079
11	18.0	1.0	2.0	10.0	1.9	1.25	9.3	3.4	4.8	0.03	4.2	8.1	6.8	15.0	10.3	5.6	57.8	0.951
26	18.0	2.0	1.0	10.0	2.0	1.34	8.7	3.8	5.4	0.03	3.6	7.3	7.7	16.4	10.7	4.7	49.9	1.130
27	18.0	2.0	1.0	20.0	1.8	1.23	8.8	3.2	4.6	0.11	4.3	8.0	6.8	15.1	10.0	5.1	51.6	1.068
31	18.0	2.0	1.5	10.0	1.9	1.25	9.3	3.4	4.9	0.03	4.2	8.1	6.8	15.0	10.3	5.6	58.0	0.948
51	18.0	3.0	1.0	10.0	1.9	1.24	9.4	3.5	5.0	0.03	4.2	8.1	6.6	15.0	10.3	5.6	58.1	0.946
129	20.0	1.0	1.0	40.0	1.9	1.30	8.9	2.8	4.0	0.46	3.8	6.7	9.0	19.7	9.5	5.0	47.9	1.246
132	20.0	1.0	1.5	20.0	2.1	1.41	9.5	3.6	5.1	0.13	3.3	6.6	9.1	19.8	10.7	5.3	56.2	1.064

TABLE 5 (CONT.)

ORIGINAL PAGE IS OF POOR QUALITY

MATERIAL: TITANIUM - 13V.11CR.3AL

HOOP THICKNESS = 0.028 HOOP WIDTH = 1.00

YOUNG'S MODULUS = 0.16E 08 YIELD STRESS = 0.25E 06

DESIGN LOAD = 40.0

HOOP DENSITY = 0.175

YIELD POINT RADIUS = 0.90

WHEEL RADIUS = 10.00

HOOP CRITERIA : SF = 2.00 . WW = 20.0

TABLE 6

WHEELS FOR THE RPI ROVER - TITANIUM

#	L	B	S	TH	RH	SF	WH	C	CO	H	LH	LW	RN	WW	LF	WF	AF	PA
1	18.0	1.0	1.0	10.0	2.2	2.40	8.0	4.1	5.8	0.03	6.3	13.1	3.8	10.4	11.0	3.7	41.0	1.229
2	18.0	1.0	1.0	20.0	2.0	2.20	8.2	3.5	4.9	0.12	7.5	14.0	3.4	9.8	10.4	4.1	43.8	1.137
3	18.0	1.0	1.0	30.0	1.8	2.05	8.2	2.9	4.2	0.25	8.7	15.5	3.2	9.5	9.7	4.0	44.1	1.123
6	18.0	1.0	1.5	10.0	2.0	2.25	8.7	3.7	5.3	0.03	7.2	14.6	3.4	9.9	10.7	4.7	49.8	1.000
7	18.0	1.0	1.0	20.0	1.9	2.06	8.8	3.1	4.4	0.11	8.6	15.1	3.1	9.3	10.1	5.1	51.1	0.965
11	18.0	1.0	2.0	10.0	1.9	2.07	9.3	3.4	4.2	0.03	9.4	16.3	3.0	9.3	10.3	5.0	57.8	0.852
26	18.0	2.0	1.0	10.0	2.0	2.24	8.7	3.9	5.4	0.03	7.2	14.6	3.4	9.8	10.7	4.7	49.9	0.998
27	13.0	2.0	1.0	20.0	1.8	2.06	8.8	3.2	4.0	0.11	9.6	16.1	3.1	9.3	10.0	5.1	51.6	0.956
31	18.0	2.0	1.5	10.0	1.9	2.09	9.3	3.4	4.9	0.03	9.4	16.3	3.0	9.3	10.3	5.0	58.0	0.850
51	18.0	3.0	1.0	10.0	1.9	2.08	9.4	3.5	5.0	0.03	8.4	16.3	3.0	9.3	10.3	5.0	58.1	0.848
126	20.0	1.0	1.0	10.0	2.4	2.72	8.7	4.7	6.6	0.04	4.9	10.9	4.9	12.7	11.7	3.1	44.0	1.182
127	20.0	1.0	1.0	20.0	2.2	2.47	8.9	4.0	5.6	0.13	5.9	12.1	4.3	11.7	11.0	4.1	48.3	1.069

TABLE 6

(CONT.)

MATERIAL: S-GLASS / EPOXY

HOOP THICKNESS = 0.055 HOOP WIDTH = 1.00

YOUNG'S MODULUS = 0.78E 07 YIELD STRESS = 0.20E 06

DESIGN LOAD = 40.0

HOOP DENSITY = 0.090

YIELD POINT RADIUS = 1.07

WHEEL RADIUS = 10.00

HOOP CRITERIA : SF = 2.50 • WW = 20.0

TABLE 7

WHEELS FOR THE RPI ROVER - S-GLASS

#	L	B	S	TH	RH	SF	WH	C	CU	H	LH	LW	BN	WM	LF	WF	AF	PA
251	22.0	1.0	1.0	10.0	2.7	2.54	9.4	5.2	7.3	0.04	14.5	33.1	1.4	7.5	12.3	3.7	48.1	0.989
376	24.0	1.0	1.0	10.0	3.0	2.81	10.0	5.8	8.1	0.05	11.9	27.9	1.7	8.3	12.8	4.0	51.5	0.738
377	24.0	1.0	1.0	20.0	2.8	2.57	10.3	5.0	7.0	0.17	14.2	32.0	1.5	7.8	12.1	4.2	57.4	0.433
381	24.0	1.0	1.5	10.0	2.9	2.68	10.7	5.4	7.7	0.04	13.1	30.3	1.6	8.0	12.6	5.0	62.2	0.772
386	24.0	1.0	2.0	10.0	2.7	2.55	11.3	5.1	7.2	0.04	14.5	33.0	1.4	7.7	12.3	5.4	72.3	0.661
401	24.0	2.0	1.0	10.0	2.9	2.68	10.7	5.5	7.7	0.04	13.1	30.4	1.6	8.0	12.5	5.7	62.3	0.770
406	24.0	2.0	1.5	10.0	2.7	2.54	11.4	5.2	7.3	0.04	14.5	33.1	1.4	7.7	12.3	5.7	72.4	0.659
426	24.0	3.0	1.0	10.0	2.7	2.54	11.4	5.2	7.3	0.04	14.5	33.1	1.4	7.7	12.3	5.7	72.6	0.658
501	26.0	1.0	1.0	10.0	3.3	3.08	10.7	6.4	8.9	0.05	9.9	23.7	2.1	9.3	13.3	6.1	54.9	0.898
502	26.0	1.0	1.0	20.0	3.0	2.81	11.0	5.5	7.7	0.18	11.9	27.5	1.8	8.6	12.5	4.1	62.0	0.735
503	26.0	1.0	1.0	20.0	2.8	2.68	11.1	4.7	6.5	0.37	13.9	30.5	1.6	8.3	11.7	5.7	64.7	0.746
506	26.0	1.0	1.5	10.0	3.2	2.95	11.4	4.0	8.4	0.05	10.8	25.7	1.9	8.9	13.1	5.1	66.1	0.740

TABLE 7

(CONT.)

ORIGINAL PAGE IS
OF POOR QUALITY

507	26.0	1.0	1.5	20.0	2.9	2.70	11.6	5.1	7.2	0.17	12.9	29.5	1.6	8.4	12.3	5.2	71.4	0.677
506	26.0	1.0	1.5	20.0	2.7	2.51	11.7	4.3	6.1	0.36	15.0	32.4	1.5	8.1	11.5	6.3	72.4	0.664
511	26.0	1.0	2.0	10.0	3.0	2.81	12.0	5.6	8.0	0.05	11.9	27.9	1.7	8.6	12.8	6.7	76.8	0.633
512	26.0	1.0	2.0	20.0	2.8	2.58	12.2	4.7	6.7	0.17	14.1	31.7	1.5	8.1	12.1	6.7	80.4	0.599
516	26.0	1.0	2.5	10.0	2.9	2.68	12.7	5.3	7.5	0.04	13.1	30.2	1.6	8.3	12.6	6.9	87.0	0.555
521	26.0	1.0	3.0	10.0	2.7	2.55	13.3	4.9	7.0	0.04	14.5	32.9	1.5	8.0	12.3	7.7	96.6	0.497
526	26.0	2.0	1.0	10.0	3.2	2.94	11.4	6.1	8.5	0.05	10.9	25.8	1.9	8.9	13.1	5.1	66.2	0.738
527	26.0	2.0	1.0	20.0	2.9	2.69	11.6	5.3	7.4	0.17	13.0	29.6	1.6	8.4	12.3	5.9	72.0	0.672
531	26.0	2.0	1.5	10.0	3.0	2.81	12.0	5.7	8.0	0.05	11.9	27.9	1.7	8.6	12.8	6.0	77.0	0.631
532	26.0	2.0	1.5	20.0	2.8	2.58	12.2	4.8	6.9	0.17	14.2	31.8	1.5	8.1	12.1	6.7	81.0	0.594
536	26.0	2.0	2.0	10.0	2.9	2.68	12.7	5.4	7.6	0.04	13.1	30.1	1.6	8.3	12.6	6.9	87.1	0.554
541	26.0	2.0	2.5	10.0	2.7	2.55	13.3	5.0	7.1	0.04	14.5	33.0	1.5	8.0	12.3	7.7	96.7	0.496
551	26.0	3.0	1.0	10.0	3.0	2.81	12.0	5.8	8.1	0.05	11.9	27.9	1.7	8.6	12.8	6.0	77.1	0.630
552	26.0	3.0	1.0	20.0	2.8	2.57	12.3	5.0	7.0	0.17	14.2	32.0	1.5	8.1	12.1	6.8	81.5	0.590
556	26.0	3.0	1.5	10.0	2.9	2.68	12.7	5.4	7.7	0.04	13.1	30.1	1.6	8.3	12.6	7.0	87.3	0.553
561	26.0	3.0	2.0	10.0	2.7	2.55	13.3	5.1	7.2	0.04	14.5	33.0	1.5	8.0	12.3	7.7	96.8	0.496
576	26.0	4.0	1.0	10.0	2.7	2.68	12.7	5.5	7.7	0.04	13.1	30.4	1.6	8.3	12.5	7.0	87.4	0.552
581	26.0	4.0	1.5	10.0	2.7	2.54	13.4	5.2	7.3	0.04	14.5	33.1	1.5	8.0	12.3	7.7	97.0	0.495
601	26.0	5.0	1.0	10.0	2.7	2.54	13.4	5.2	7.3	0.04	14.5	33.1	1.4	8.0	12.3	7.7	97.1	0.494

TABLE 7

(CONT.)

much promise at a thickness of 0.055 inches. With band numbers down to 1.4 a one band solution, 1.4 inches wide, is obtainable, while wheel efficiency runs close to 6.0. Future work with different materials will eventually lead to even better solutions if the right combination of material properties are obtained. Since the stresses are proportional to the product, $E t$, and the wheel load is proportional to the product, $E t^3$, one should search for a very flexible material with a high yield strength and low density.

If, for example, the elastic modulus is lower by 50% then the thickness can be doubled resulting in a wheel which can carry four times the load. Likewise, if the yield strength is doubled then the thickness can again be doubled affording eight times the carrying capacity. The proper combination of properties will therefore yield an inverted wheel which is far superior to those depicted throughout Tables 5 to 7.

7.2 Wheels for the Proposed Mars Roving Vehicle

As discussed previously, the proposed Mars vehicle will impose an axle load of approximately 140 pounds. The chosen wheel radius was 15 inches with the hoop parameters in the following range:

Hoop Length, $L = 26.0$ to 34.0 inches

Base Length, $B = 1.0$ to 5.0 inches

Flange Length, $S = 1.0$ to 3.0 inches

Flange Angle, $\Theta = 10^\circ$ to 50°

The thicknesses used were the same as those previously, thus they are not the optimum for this vehicle. The safety factor was set very high at 2.5 while the efficiency had a lower bound of five. With these requirements a number of solutions, with Beta Titanium, are obtained as shown in Table 8. Although the band numbers are very high they can be

MATERIAL: TITANIUM - 13V.11CR.3AL

HOOP THICKNESS = 0.028 HCCP WIDTH = 1.00

YOUNGS' MODULUS = 0.16E 08 YIELD STRESS = 0.25 CG

DESIGN LOAD = 140.0

HOOP DENSITY = 0.175

YIELD POINT RADIALS = 0.90

WHEEL RADIUS = 15.00

HOOP CRITERIA : SF = 2.50 . WW = 28.0

TABLE 8

WHEELS FOR THE PROPOSED POWER - TITANIUM

	L	B	S	TH	RH	SF	WH	C	CO	H	LH	LW	BN	WN	LF	WF	AF	PA
1	26.0	1.0	1.0	10.0	3.3	3.68	10.7	6.4	8.9	0.05	2.7	5.7	29.1	27.5	16.7	4.1	62.8	2.435
2	26.0	1.0	1.0	20.0	3.0	3.37	11.0	5.5	7.7	0.18	3.2	6.3	25.6	21.8	15.7	4.9	77.5	2.127
3	26.0	1.0	1.0	30.0	2.8	3.12	11.1	4.7	6.6	0.37	3.8	6.7	23.8	23.4	14.6	5.5	80.7	2.027
4	26.0	1.0	1.0	40.0	2.6	2.92	11.1	4.0	5.6	0.61	4.3	6.8	23.7	23.3	13.5	5.9	79.8	2.040
5	26.0	1.0	1.0	50.0	2.5	2.77	11.0	3.3	4.7	0.89	4.8	6.4	25.3	24.6	12.6	6.1	76.4	2.154
6	26.0	1.0	1.5	10.0	3.2	3.53	11.4	6.0	8.4	0.05	2.9	6.1	26.9	25.8	16.4	5.1	82.8	2.003
7	26.0	1.0	1.5	20.0	2.9	3.23	11.6	5.1	7.2	0.17	3.5	6.7	23.9	23.5	15.4	5.8	81.2	1.833
8	26.0	1.0	1.5	30.0	2.7	3.00	11.7	4.3	6.1	0.36	4.0	7.1	22.5	22.4	14.3	6.3	90.2	1.862
9	26.0	1.0	1.5	40.0	2.5	2.83	11.6	3.5	5.1	0.59	4.6	7.0	22.7	22.6	13.3	6.0	82.1	1.999
10	26.0	1.0	1.5	50.0	2.4	2.69	11.5	2.8	4.2	0.86	5.0	6.5	24.7	24.2	12.4	6.0	90.1	1.709
11	26.0	1.0	2.0	10.0	3.0	3.37	12.0	5.6	8.0	0.05	3.2	6.5	24.8	24.2	16.0	6.0	100.3	1.617
12	26.0	1.0	2.0	20.0	2.8	3.09	12.2	4.7	6.7	0.17	3.8	7.1	22.3	22.2	15.1	6.7	100.3	1.617

ORIGINAL PAGE IS
OF POOR QUALITY

TABLE 8

(CONT.)

365	30.0	5.0	2.0	50.0	2.3	2.62	15.9	3.3	3.6	0.84	5.3	6.6	24.7	27.1	12.2	11.2	136.5	1.224
366	30.0	5.0	2.5	10.0	2.9	3.21	16.7	5.3	7.5	0.04	3.5	7.0	23.4	25.9	15.7	10.9	171.5	0.967
367	30.0	5.0	2.5	20.0	2.6	2.96	16.8	4.3	6.2	0.16	4.2	7.6	21.1	23.9	14.8	11.5	169.9	0.965
368	30.0	5.0	2.5	30.0	2.5	2.77	16.8	3.4	5.1	0.33	4.8	7.8	20.5	23.3	13.8	11.8	163.1	1.001
369	30.0	5.0	2.5	40.0	2.4	2.64	16.6	2.6	4.0	0.55	5.2	7.5	21.4	24.2	12.9	11.9	153.0	1.073
370	30.0	5.0	2.5	50.0	2.3	2.54	16.3	1.8	3.1	0.81	5.6	6.7	24.3	26.7	12.1	11.7	141.1	1.181
371	30.0	5.0	3.0	10.0	2.7	3.05	17.3	4.9	7.0	0.04	3.9	7.5	21.5	24.2	15.3	11.9	181.9	0.903
372	30.0	5.0	3.0	20.0	2.5	2.82	17.4	3.9	5.7	0.15	4.6	8.1	19.7	22.6	14.4	12.4	172.5	0.911
373	30.0	5.0	3.0	30.0	2.4	2.65	17.3	2.9	4.5	0.32	5.2	8.2	19.4	22.3	13.5	12.6	170.2	0.954
374	30.0	5.0	3.0	40.0	2.3	2.54	17.1	2.1	3.5	0.53	5.7	7.8	20.7	23.5	12.7	12.5	158.6	1.030
473	32.0	4.0	3.0	30.0	2.7	3.06	17.4	3.6	5.5	0.37	3.9	6.9	23.8	27.7	14.5	11.9	172.6	0.972
493	32.0	5.0	2.5	30.0	2.7	3.04	17.5	3.8	5.7	0.36	4.0	7.0	23.6	27.5	14.4	12.1	173.8	0.964
494	32.0	5.0	2.5	40.0	2.6	2.88	17.3	3.0	4.6	0.60	4.4	6.9	24.0	27.9	13.5	12.2	163.5	1.027
497	32.0	5.0	3.0	20.0	2.8	3.11	18.1	4.4	6.4	0.17	3.8	7.1	23.1	27.0	15.1	12.5	189.6	0.881
498	32.0	5.0	3.0	30.0	2.6	2.92	18.0	3.4	5.2	0.35	4.3	7.3	22.3	26.2	14.2	12.8	181.4	0.910
499	32.0	5.0	3.0	40.0	2.5	2.79	17.8	2.5	4.0	0.58	4.7	7.1	23.0	27.0	13.2	12.8	160.6	0.984

TABLE 8 (CONT.)

easily lowered by doubling the hoop thickness which multiples the wheel support by a factor of eight. This will result in two banded solutions, 1.5 inches wide, at a sacrifice of safety with the resulting factor equal to 1.25. On the other hand, S-Glass/Epoxy as shown in Table 9, has a minimum efficiency of 10, a band number correctable to less than one with numerous solutions having safety factors of approximately 1.4. Even though this material is seen to yield satisfactory wheels, as stated before, far superior wheels can be obtained with the proper combination of materials.

MATERIAL: S-GLASS / EPOXY

HCCP THICKNESS = 0.055 HCCP WIDTH = 1.00

YOUNG'S MODULUS = 0.78E 07 YIELD STRESS = 0.20E 06

DESIGN LOAD = 140.0

HCCP DENSITY = 0.090

YIELD POINT RADIUS = 1.07

WHEEL RADIUS = 15.00

HCCP CRITERIA ; SF = 2.50 , WW = 14.0

TABLE 9

WHEELS FOR THE PROPOSED COVER - S-GLASS

	L	B	S	TH	RT	SF	WH	C	CO	H	LH	LW	BN	NW	LF	WF	AF	PA
1	26.0	1.0	1.0	10.0	1.3	7.08	10.7	6.4	8.9	0.05	9.9	20.9	7.1	10.5	16.7	4.1	68.8	2.188
2	26.0	1.0	1.0	20.0	3.0	2.81	11.0	5.5	7.7	0.18	11.9	23.4	6.3	9.9	15.7	4.9	77.5	1.935
3	26.0	1.0	1.0	30.0	2.8	2.60	11.1	4.7	6.6	0.37	13.9	24.9	5.9	9.6	14.6	5.5	80.7	1.855
6	26.0	1.0	1.5	10.0	3.2	2.95	11.4	6.0	8.4	0.05	10.8	22.4	6.6	10.1	16.4	5.1	82.8	1.814
7	26.0	1.0	1.5	20.0	2.9	2.70	11.6	5.1	7.2	0.17	12.9	24.8	5.9	9.6	15.4	5.8	89.2	1.678
8	26.0	1.0	1.5	30.0	2.7	2.51	11.7	4.3	6.1	0.36	15.0	26.1	5.6	9.4	14.3	6.3	90.2	1.657
11	26.0	1.0	2.0	10.0	3.0	2.81	12.0	5.6	8.0	0.05	11.9	24.0	6.1	9.8	16.0	6.0	96.1	1.559
12	26.0	1.0	2.0	20.0	2.8	2.58	12.2	4.7	6.7	0.17	14.1	26.4	5.5	9.3	15.1	6.7	100.3	1.489
16	26.0	1.0	2.5	10.0	2.9	2.68	12.7	5.3	7.5	0.04	13.1	25.8	5.7	9.4	15.7	6.9	108.7	1.375
21	26.0	1.0	3.0	10.0	2.7	2.55	13.3	4.9	7.0	0.04	14.5	27.7	5.3	9.1	15.3	7.9	120.6	1.237
26	26.0	2.0	1.0	10.0	3.2	2.94	11.4	6.1	8.5	0.05	10.9	22.4	6.6	10.1	16.4	5.1	83.0	1.809
27	26.0	2.0	1.0	20.0	2.9	2.69	11.6	5.3	7.4	0.17	13.0	24.9	5.9	9.6	15.4	5.9	89.9	1.664

TABLE 0

(CONT.)

ORIGINAL PAGE IS
OF POOR QUALITY

458	32.0	4.0	1.5	30.0	3.0	2.84	15.7	4.9	7.0	0.41	11.6	22.1	6.7	11.5	15.2	9.6	146.7	1.033
459	32.0	4.0	1.5	40.0	2.9	2.67	15.7	4.1	5.9	0.67	13.2	22.5	6.6	11.4	14.1	10.0	141.1	1.073
460	32.0	4.0	1.5	50.0	2.7	2.54	15.6	3.3	4.8	0.97	14.5	21.7	6.8	11.6	13.1	10.1	132.7	1.142
461	32.0	4.0	2.0	10.0	3.4	3.21	16.0	6.5	9.2	0.05	9.1	19.5	7.7	12.4	17.1	9.1	155.8	0.978
462	32.0	4.0	2.0	20.0	3.2	2.95	16.2	5.5	7.8	0.19	10.8	21.8	6.8	11.6	16.0	9.9	151.0	0.954
463	32.0	4.0	2.0	30.0	2.9	2.75	16.3	4.5	6.5	0.39	12.5	23.2	6.4	11.2	15.0	10.4	155.7	0.971
464	32.0	4.0	2.0	40.0	2.8	2.59	16.2	3.6	5.3	0.65	14.0	23.3	6.3	11.1	13.9	10.6	148.2	1.020
466	32.0	4.0	2.5	10.0	3.3	3.06	16.7	6.1	8.7	0.05	9.9	20.8	7.1	11.9	16.7	10.1	168.5	0.901
467	32.0	4.0	2.5	20.0	3.0	2.83	16.9	5.0	7.3	0.18	11.7	23.1	6.4	11.2	15.7	10.8	169.6	0.892
468	32.0	4.0	2.5	30.0	2.8	2.65	16.9	4.1	6.0	0.38	13.4	24.3	6.1	10.9	14.7	11.2	164.4	0.918
469	32.0	4.0	2.5	40.0	2.7	2.51	16.7	3.2	4.8	0.63	14.9	24.2	6.1	10.9	13.7	11.3	155.1	0.973
471	32.0	4.0	3.0	10.0	3.2	2.95	17.3	5.8	8.2	0.05	10.8	22.3	6.7	11.4	16.4	11.0	180.6	0.829
472	32.0	4.0	3.0	20.0	2.9	2.72	17.5	4.6	6.8	0.18	12.7	24.5	6.0	10.8	15.4	11.6	171.6	0.840
473	32.0	4.0	3.0	30.0	2.7	2.55	17.4	3.6	5.5	0.37	14.4	25.6	5.8	10.6	14.5	11.9	172.6	0.872
476	32.0	5.0	1.0	10.0	3.6	3.34	15.4	6.9	9.7	0.05	8.4	18.3	8.2	12.9	17.4	8.2	142.6	1.072

TABLE 19

(CONT.)

611	34.0	5.0	2.0	10.0	3.6	3.35	17.4	6.8	9.5	0.05	8.4	18.2	8.2	13.4	17.4	10.2	176.9	0.867
612	34.0	5.0	2.0	20.0	3.3	3.07	17.6	5.7	8.1	0.20	10.0	20.5	7.3	12.5	16.3	11.0	179.7	0.848
613	34.0	5.0	2.0	30.0	3.1	2.86	17.7	4.7	6.8	0.41	11.5	21.9	6.8	12.0	15.2	11.5	175.7	0.865
614	34.0	5.0	2.0	40.0	2.9	2.70	17.6	3.8	5.6	0.68	12.9	22.2	6.7	11.8	14.2	11.8	167.2	0.908
615	34.0	5.0	2.0	50.0	2.8	2.58	17.3	3.0	4.5	0.99	14.2	21.4	7.0	12.1	13.2	11.8	156.1	0.975
616	34.0	5.0	2.5	10.0	3.4	3.22	18.0	6.4	9.1	0.05	9.1	19.5	7.7	12.9	17.1	11.1	189.7	0.806
617	34.0	5.0	2.5	20.0	3.2	2.96	18.2	5.3	7.6	0.19	10.8	21.7	6.9	12.0	16.0	11.9	190.3	0.799
618	34.0	5.0	2.5	30.0	3.0	2.76	18.2	4.3	6.3	0.40	12.3	23.0	6.5	11.6	15.0	12.3	184.4	0.822
619	34.0	5.0	2.5	40.0	2.8	2.62	18.1	3.4	5.1	0.66	13.7	23.1	6.4	11.6	14.0	12.4	174.0	0.871
620	34.0	5.0	2.5	50.0	2.7	2.51	17.7	2.5	4.0	0.96	14.9	21.9	6.8	11.9	13.1	12.5	161.3	0.942
621	34.0	5.0	3.0	10.0	3.3	3.08	18.7	6.0	8.6	0.05	9.5	20.8	7.2	12.3	16.7	12.1	201.8	0.755
622	34.0	5.0	3.0	20.0	3.0	2.84	18.8	4.9	7.1	0.18	11.6	23.0	6.4	11.6	15.8	12.7	200.4	0.756
623	34.0	5.0	3.0	30.0	2.9	2.66	18.8	3.8	5.8	0.38	13.2	24.1	6.1	11.3	14.8	13.1	192.6	0.786

TABLE 9 (CONT.)

PART 8

DISCUSSIONS AND CONCLUSION

As demonstrated previously, an inverted toroidal wheel can be synthesized for any vehicle, if the described derivation is employed. Whether or not the result is the optimum mobility concept, for a particular vehicle subjected to a given array of terrains, proves to be another question. The answer to this would only come from a comparison of the various mobility systems in their final form. To meet this challenge the search for superior materials; i.e. of very low elastic moduli, low densities, and of very high yield strengths; must continue. Composites, which may be "tailored" for various applications, seem to be the most promising materials with which to meet these special needs.

Future work must include the "cleaning up" of the few but important assumptions made in the derivation, namely that:

1. The bending moment is zero at the lower cross-section in Figures 26A, B and 27.
2. The peripheral hoops deflect only in their own plane.
3. The circular region is truly circular.
4. The grouser does not affect the load carrying capability.

Other areas of interest are the response of the wheel when subjected to dynamic loads and an assessment of the adverse affect of such loads on wheel life. The extension of the derivation into the dynamic region is also desirable. A method of determining wheel life for composite wheels is needed, as the S-N/Goodman technique applies only to steel. Much work will have to be done concerning the hoop-spoke interface if composite hoops are used, which leads to the interesting idea of a lightweight

composite hub as well. The investigation of wheels with more than sixteen hoops covering the hub can easily be investigated with the limiting case being a continuous inverted hoop or an "inverted shell".

The inverted toroidal wheel, as presently formulated, is in a class of so-called advanced mobility systems. This exceptional wheel, as improved by the proposed future research, will prove to be one of the very few concepts which will meet the extremely stringent requirements imposed by the Martian terrain.

PART 9

LITERATURE CITED

1. Simon, R. L., "Design of a Toroidal Wheel for a Martian Roving Vehicle." Master's Thesis, Rensselaer Polytechnic Institute, May 1971.
2. Lipowicz, R. F., "A Wheel Design Analysis and Locomotion Study for the RPI-Mars Roving Vehicle." Master's Thesis, Rensselaer Polytechnic Institute, May 1976.
3. Bekker, M. G., Off-The-Road Locomotion, The University of Michigan Press, 1960.
4. Timoshenko, S., Strength of Materials, Volume I, Elementary Theory and Problems, 3rd Edition, 1955.
5. Shigley, J. E., Mechanical Engineering Design, 2nd Edition, 1972.
6. Clark, D. S., and Varney, W. R., Physical Metallurgy, 1962.
7. Jones, R. M., Mechanics of Composite Materials, 1975.

APPENDIX A

INVERTED TOROIDAL WHEEL PROGRAM

/JOB \$\$\$\$\$\$ KOSKOL

C
C
C
C
C
C
C
C
C
C
C

THIS PROGRAM UTILIZES THE INVERTED TORROIDAL HOOP-SPOKE DERIVATION
TO SEARCH FOR ACCEPTABLE WHEEL DESIGNS. THE INPUT VALUES (HOOP
LENGTH, BASE LENGTH, FLANGE LENGTH, & FLANGE ANGLE) ARE
INCREMENTED AFTER EACH TRAIL. AN ACCEPTABLE WHEEL DESIGN IS ONE
WHOSE PARAMETERS SATISFY THE GIVEN CRITERIA. (SEE BELOW)

**ORIGINAL PAGE IS
OF POOR QUALITY**

1
2

REAL L,LOR,INER,MCM,LOAD
INTEGER HOOP

C
C
C
C
C
C

INITIAL INPUT PARAMETERS AND THEIR
RESPECTIVE INCREMENTS ARE ENTERED.

3

READ(5,13)LCR,DL,BOR,DB,SOR,JS,THCR,DTH

C
C
C
C
C
C

THE NUMBER OF TRAILS PER PARAMETER & THE INITIAL
TRAIL NUMBER ARE ENTERED.

4

READ(5,14)N,HUOP

C
C
C
C
C
C

CRITERIA LIMITS ARE ENTERED. I.E.: SAFETY FACTOR, MIN. =;
WHEEL WEIGHT, MAX. =.

5

READ(5,100)SF,WW

C
C
C
C
C
C

THE WEIGHT THAT THE WHEEL WILL SUPPORT IS ENTERED. (AXLE LOAD).

6

READ(5,700)DESLD

C
C
C
C
C
C

MATERIAL DENSITY IS ENTERED.

7

READ(5,203)RHO

C
C
C
C
C
C

HOOP PROPERTIES AND DIMENSIONS ALONG WITH THE
WHEEL RADIUS ARE ENTERED.

8

READ(5,20)E,SIGYP,WIDTH,WRAD

9

READ(5,501)THICK

10

PI=3.1415927

11

NCOUNT=0

C
C

C AREA MOMENT OF INERTIA AND YIELD POINT RADIUS ARE CALCULATED.

C

```
12 INER=(THICK**3)*WIDTH/12.  
13 RYP=(E*THICK)/(SIGYP*2.)
```

C
C
C
C
C

C

ALL INPUT INFORMATION AND HEADINGS ARE PRINTED.

```
14 WRITE(6,202)  
15 WRITE(6,200)  
16 WRITE(6,24)THICK,WIDTH  
17 WRITE(6,500)E,SIGYP  
18 WRITE(6,600)  
19 WRITE(6,701)DESLO  
20 WRITE(6,201)RHC  
21 WRITE(6,25)RYP  
22 WRITE(6,50)WRAD  
23 WRITE(6,102)SF,WW  
24 WRITE(6,202)  
25 WRITE(6,91)
```

**ORIGINAL PAGE IS
OF POOR QUALITY**

26 PRINT,' HOOP #, HOOP LENGTH, BASE LENGTH, FLANGE LENGTH, FLANGE AN
GLE, RADIUS.'

```
27 WRITE(6,60)  
28 PRINT,' FACTOR OF SAFETY, WIDTH, STATIC CLEARANCE, NO LOAD CLEARAN  
&CE, HEIGHT.'
```

```
29 WRITE(6,60)  
30 PRINT,' HOOP LOAD, WHEEL LOAD, NUMBER OF BANDS, WHEEL WEIGHT, FOOT  
&PRINT LENGTH.'
```

```
31 WRITE(6,60)  
32 PRINT,' FOOTPRINT WIDTH, FOOTPRINT AREA, & AVEPAGE PRESSURE; RESPE  
&CTIVELY.'
```

```
33 WRITE(6,600)  
34 PRINT,' N L B S TH RH SF WH C CO H LM LW  
& BN WW LF WF AF PA '  
35 WRITE(6,60)
```

C
C
C
C
C

C

THE FOLLOWING FOUR DO-LOOPS INCREMENT THE INPUT PARAMETERS.

```
36 DO 4 I=1,N  
37 IF(I.EQ.1)GO TO 8  
38 L=L+DL  
39 GO TO 16  
40 8 L=LOR  
41 16 CONTINUE  
42 DO 5 J=1,N  
43 IF(J.EQ.1)GO TO 9  
44 B=B+DB  
45 GO TO 17  
46 9 B=BOR  
47 17 CONTINUE  
48 DO 6 K=1,N  
49 IF(K.EQ.1)GC TO 10  
50 S=S+DS  
51 GO TO 19  
52 10 S=SOR
```

```

53      18 CONTINUE
54      DO 7 M=1,N
55      IF(M.EQ.1)GO TO 11
56      TH=TH+DTH*PI/180.
57      GO TO 19
58      11 TH=THOR*PI/180.
59      19 CONTINUE
60      STH=SIN(TH)
61      CTH=COS(TH)
62      HOOP=HOOP+1

      C
      C -----
      C ALL HOOP OUTPUTS ARE CALCULATED.
      C -----
      C
63      R=(L/2-B/2-S*CTH)/(STH+PI+TH)
64      W=2*(1+STH)*R+B+S*CTH*2
65      C=R*(1.+CTH)-S*STH
66      HACT=R*(1.-CTH)
67      G=B/2+S*CTH+R*STH
68      WF=2*G
69      MOM=E*INER/R
70      LOAD=MOM/R
71      P=MOM/(2*R)
72      SAFETY=P/RYP
73      SPRGK=((E*INER)/(R**3))/((PI-2)/2+TH/2-(STH*CTH)/2-(STH**2)/2+CTH)
74      DEFL=P/SPRGK
75      CD=C+DEFL

      C
      C -----
      C THE CONTRIBUTION OF PERIPHERAL HOOPS IS CALCULATED.
      C -----
      C
76      AUXHPS=0.
77      DO 31 IS=1,6
78      CHECK=(COS(22.5*(PI/180.)*IS)-1)*WRAD+DEFL
79      IF(CHECK.LE.0)ME=IS-1
80      IF(CHECK.LE.0)GO TO 34
81      31 CONTINUE
82      34 CONTINUE
83      IF(ME.EQ.0)GO TO 32
84      DO 30 IT=1,ME
85      AUXHPS=2*((COS(22.5*(PI/180.)*IT)-1)*WRAD+DEFL)+AUXHPS
86      30 CONTINUE
87      32 CONTINUE

      C
      C -----
      C ALL WHEEL OUTPUTS ARE CALCULATED.
      C -----
      C
88      WHLOAD=2*SPRGK*(DEFL+AUXHPS)
89      WTHOOP=16.*RMO*L*THICK*WIDTH
90      IF(WTHOOP.EQ.WHLOAD)GO TO 112
91      BANDS=(DESLD+5.)/(WHLOAD-WTHOOP)
92      GO TO 133
93      112 BANDS=1000000.0
94      133 CONTINUE
95      WEIGHT=5.+WTHOOP*BANDS
96      FPLTH=2*DEFL*SQRT(2*WRAD/DEFL-1)

```

```

97      FPAREA=FPLTH*WF
98      IF(WF.LE.0)GO TO 22
99      FPAVPR=(DESLD*WEIGHT)/FPAREA
100     GO TO 23
101     22 FPAVPR=1000000.0
102     23 CONTINUE

C
C
C      -----
C      THE TRAIL WHEEL IS CHECKED TO DETERMINE IF IT SATISFIES
C      THE CRITERIA OF SAFETY FACTOR AND WEIGHT.
C      -----
C

103     IF(SAFETY.GE.SF.AND.WEIGHT.LE.WW)GO TO 110
104     GO TO 111
105     110 IF(WEIGHT.GE.0)GO TO 80
106     111 CONTINUE
107     GO TO 90

C
C
C      -----
C      A WHEEL IS O.K.'ED AND ITS ENTIRE INPUT
C      & OUTPLT SPECIFICATIONS ARE PRINTED.
C      -----
C

108     80 CONTINUE
109     TH=TH*180./PI
110     WRITE(6,2)HCOP,L,B,S,TH,R,SAFETY,W,C,CO,HACT,LOAD,WPLD,BANDS,WFI
      &GHT,FPLTH,WF,FPAREA,FPAVPR
111     TH=TH*PI/180.
112     NCOUNT=NCOUNT+1
113     90 CONTINUE
114     7 CONTINUE
115     6 CONTINUE
116     5 CONTINUE
117     4 CONTINUE
118     IF(NCOUNT.EQ.1)GO TO 601
119     WRITE(6,400)NCOUNT
120     GO TO 602
121     601 CONTINUE
122     WRITE(6,600)
123     WRITE(6,604)NCOUNT
124     602 CONTINUE
125     WRITE(6,300)

C
C
C      -----
C      THE NUMBER OF SOLUTIONS FOR THIS RUN IS PRINTED.
C      -----
C

126     2 FORMAT(1X,I3,F5.1,2F4.1,F5.1,F4.1,F5.2,F5.1,2F4.1,F5.2,7F5.1,F6.3
      &,/)
127     13 FORMAT(3F5.2)
128     14 FORMAT(2I5)
129     20 FORMAT(4F15.3)
130     24 FORMAT(15X,16H HOOP THICKNESS =,F6.3,3X,12H HOOP WIDTH =,F6.2,/////)
131     25 FORMAT(15X,20H YIELD POINT RADIUS =,F5.2,/////)
132     50 FORMAT(15X,14H WHEEL RADIUS =,F5.2,/////)
133     50 FORMAT(/)
134     91 FORMAT(5X,61H*****THE FOLLOWING WHEELS SATISFY THE SF & WW CRITER
      &IA*****,/////)
135     100 FORMAT(F5.1,F ..)

```

```

136 102 FORMAT(15X,20HHCOP CRITERIA ; SF =.F5.2,7H . WW =.F5.1)
137 200 FORMAT(15X,34HMATERIAL: TITANIUM - 13V,11CR,3AL,//////)
138 201 FORMAT(15X,14HHCOP DENSITY =.F6.3,//////)
139 202 FORMAT(1H1,//////)
140 203 FORMAT(F10.2)
141 300 FORMAT(1H1)
142 400 FORMAT(//////,5X,16H*****THERE ARE .13.17H SCLUTIONS*****)
143 500 FORMAT(15X,17HYOUNGS' MODULUS =.E10.2,3X,14HYIELD STRESS =.E1
144 501 FORMAT(F15.3)
145 600 FORMAT(//////)
146 604 FORMAT(5X,14H*****THERE IS.12.15H SCLUTION*****)
147 700 FORMAT(F15.2)
148 701 FORMAT(15X,13HDESIGN LOAD =.F5.1,//////)
149 STOP
150 END

```

/RUN

APPENDIX B

BANDS PROGRAM

/JOB \$\$\$\$\$\$ KOSKOL

C
C
C
C
C
C
C
C
C
C
C
C

GIVEN SIX INPUT PARAMETERS (HOOP LENGTH, BASE LENGTH, FLANGE LENGTH, FLANGE ANGLE, HOOP THICKNESS, & THE NUMBER OF BANDS) THIS PROGRAM FINDS THE CHANGE IN LENGTH, LENGTH (FOR A PRESS FIT), & MANUFACTURING LENGTH TO PROHIBIT INTERFERENCE; FOR EACH BAND OF A MULTI-HOOP SYSTEM.

```

1 DIMENSION L(19),R(19),DELTA(19),DELMAN(19),LMAN(19)
2 REAL LDES,L,LMAN
3 READ(5,1)LOES,S,TH,THICK,N
4 WRITE(6,10)LDES,B
5 WRITE(6,20)S,TH
6 WRITE(6,30)THICK,N
7 PI=3.1415927
8 TH=TH*PI/180.
9 RDES=(LDES/2-B/2-S*COS(TH))/(SIN(TH)+PI+TH)
10 DO 3 IA=1,N
11 R(IA)=RDES+THICK*(FLOAT(IA)-(FLOAT(N)+1)/2)
12 L(IA)=2*(R(IA)*(SIN(TH)+PI+TH)+B/2+S*COS(TH))
13 DELTA(IA)=L(IA)-LDES
14 DELMAN(IA)=3.*DELTA(IA)
15 LMAN(IA)=LDES+DELMAN(IA)
16 WRITE(6,6):A,DELTA(IA),L(IA),LMAN(IA)
17 3 CONTINUE
18 WRITE(6,100)
19 1 FORMAT(4F5.1,F6.4,I5)
20 6 FORMAT(2X,15HBRAND NUMBER =,I3,12X,15HLENGTH CHANGE =,F6.2,/,7X,5HL
LENGTH =,F6.2,12X,22HMANUFACTURING LENGTH =,F6.2,/)
21 10 FORMAT(1H1,1X,15HDESIGN LENGTH =,F6.1,4X,13HBASE LENGTH =,F4.1,/)
22 20 FORMAT(2X,15HFLANGE LENGTH =,F4.1,9X,14HFLANGE ANGLE =,F5.1,/)
23 30 FORMAT(2X,11HTHICKNESS =,F5.3,11X,17HNUMBER OF BANDS =,I3,/)
24 100 FORMAT(1H1)
25 STOP
26 END

```

/RUN

SN 4 DATE
Filmed

DEC 22 1974